Cover Page

INTERNATIONAL JOURNAL OF MULTIDISCIPLINARY EDUCATIONAL RESEARCH
ISSN:2277-7881; IMPACT FACTOR :8.017(2023); IC VALUE:5.16; ISI VALUE:2.286
Peer Reviewed and Refereed Journal: VOLUME:12, ISSUE:7(5), July: 2023
Online Copy of Article Publication Available (2023 Issues)
Scopus Review ID: A2B96D3ACF3FEA2A
Article Received: 2nd July 2023
Publication Date:30th July 2023
Publisher: Sucharitha Publication, India
Digital Certificate of Publication: www.ijmer.in/pdf/e-CertificateofPublication-IJMER.pdf

DOI: http://ijmer.in.doi./2023/12.07.88
www.ijmer.in

LUNG SOUND DETECTION OF RESPIRATORY DISEASES (SCMC APPROACH)

[a]Atanu Manna and [b]Dr.Kamal Kr. Srivastava

[A] Research Scholar, Department of Computer Science and Engineering, Mansarovar Global University Madhya Pradesh India
[B] Professor, Department of Computer Science And Engineering,Mansarovar Global University Madhya Pradesh India

Abstract:

The overall structure of LS detection system of pulmonary diseases has a front-end feature extraction phase and a back-end classifier phase. Most automatic identification systems of pulmonary diseases from LS are devoted on characterizing the breathing sound for the front-end feature extraction with different classification models.With the recent progress in digital signal processing and machine learning technologies, the electronic stethoscope has been used to replace the traditional acoustic stethoscope in recording LS. Recent works have reported the success of spectral centroid-based features for many speech detection applications. However, spectral centroid-based features for lung sound (LS) detection of pulmonary diseases have received less attention. In this paper, Spectral Centroid Magnitude Coefficients (SCMC) which is a type of spectral centroid-based features, is explored for LS detection of pulmonary diseases. Additionally, Thomson multi-taper (TMT) method is introduced to replace single taper method in order to reduce large variance representation of the original SCMC feature. We denote this modified SCMC feature as multi-taper SCMC (TMT-SCMC) feature. The performance of the proposed SCMC features is investigated using LS signals provided by a publicly available database. The experimental results demonstrate that the SCMC with a proper frame length and the optimal number of sub-bands provided the accuracy values of 91.98%, 96.48%, 98.35%.

Keywords: Biosensor Signal Processing; Spectral Centroid-Based Feature; Multi-Taper Method;Pulmonary Diseases

1. Introduction

Lung sound (LS) signals provide important clues in diagnosing pulmonary dis-eases [1]. The most popular diagnostic method for pulmonary diseases used by specialists is based on auscultation of the LS with a stethoscope [2]. However, auscultation using traditional stethoscope may be wrong because of the following factors: (a) human ear is sensitive to the frequency range of 1000Hz to 2000Hz, so that important information in the LS frequency range from 100Hz to 1000Hz may be lost and (b) in-experienced medical staff leading to inaccurate diagnosis of diseases. To solve the problems mentioned above, alternative auscultation method is required to assist doctors for better prediction of pulmonary diseases. With the recent progress in digital signal processing and machine learning technologies, the electronic stethoscope has been used to replace the traditional acoustic stethoscope in recording LS The recorded LS signals can be extracted as a new representation via digital signal processing and it can be recognized by contracting ma-chine learning model [3]. Building a LS detection system for pulmonary diseases by exploiting digital signal processing and machine learning techniques based on LS signals obtained by the electronic stethoscope has been shown to be effective in detecting pulmonary diseases [4]. In this paper, we focus on LS detection based on digital signal processing and machine learning technologies to detect pulmonary diseases, which is a subject area of pattern recognition task in the fields of biosensors and computer science.

The overall structure of LS detection system of pulmonary diseases has a front-end feature extraction phase and a back-end classifier phase. Most automatic identification systems of pulmonary diseases from LS are devoted on characterizing the breathing sound for the front-end feature extraction with different classification models. Previous studies have reported the exploitation of wavelet-based features at the feature extraction stage [5,6,7], Mel frequency cepstral coefficients (MFCC) [8], linear predictive cepstral coefficient [9], bispectrum [8] and the

Cover Page

INTERNATIONAL JOURNAL OF MULTIDISCIPLINARY EDUCATIONAL RESEARCH
ISSN:2277-7881; IMPACT FACTOR :8.017(2023); IC VALUE:5.16; ISI VALUE:2.286
Peer Reviewed and Refereed Journal: VOLUME:12, ISSUE:7(5), July: 2023
Online Copy of Article Publication Available (2023 Issues)
Scopus Review ID: A2B96D3ACF3FEA2A
Article Received: 2nd July 2023
Publication Date:30th July 2023
Publisher: Sucharitha Publication, India
Digital Certificate of Publication: www.ijmer.in/pdf/e-CertificateofPublication-IJMER.pdf

DOI: http://ijmer.in.doi./2023/12.07.88
www.ijmer.in

Empirical Wavelet Transform (EWT) with Fixed Boundary Points (EWT-FBP) feature [10]. Most previous studies [5,9,11-14] have applied Support Vector Machine (SVM) as a classifier to identify pulmonary diseases from LS because it can efficiently distinguish the data of different classes based on an optimal hyperplane with the biggest possible margin. In addition to using SVM, there are various classifiers such as Gaussian mixture model (GMM) [15], k-nearest neighbor (KNN) [14], Linear discriminant analysis (LDA) [14], Decision trees (DT) [14], multilayer perceptron (MLP) [10], random forest (RF) [10], extreme gradient boosting (XGBoost) [10], and light gradient boosting machine (LGBM) [10] classifiers. From the aforementioned classifiers, it can be seen that the ability to classify pulmonary diseases from LS signals is significantly influenced by the effectiveness of feature extraction. This suggests that the exploration/design of efficient feature extraction is important in achieving expected results for automatic identification of pulmonary diseases. Apart from the classifiers mentioned above, deep neural network (DNN) methods have been proven to be efficient in identifying pulmonary diseases. The authors of [16] proposed convolutional neural network (CNN) with MFCC information. The experimental results showed that the exploitation of the CNN with MFCC information provided promising results for the classification for normal versus asthma versus pneumonia. The combination of VGGish network with the bidirectional gated recur-rent unit neural network (BiGRU) was proposed in [17]. The results exhibited that VGGish BiGRU using Mel-spectrogram was superior to CNN using MFCC because of the fused advantages of VGGish and BiGRU. Although these methods can efficiently classify pulmonary diseases from LS signals, the classification performance strongly requires a large number of training data for deep neural network training. Unfortunately, most of the publicly accessible LS dataset is not large enough to guarantee results for DNN-based diagnosis of pulmonary diseases.

In this paper, spectral centroid-based feature is applied for automatic LS identification of pulmonary diseases. Recently, Spectral Centroid Magnitude Coefficients (SCMC) feature has been proven to be efficient for many speech applications such as speaker verification [18,19], replay attack detection [20], cognitive load classification [21] and speech emotion recognition [22]. We therefore hypothesize that the SCMC, as a spectral centroid-based feature, is useful for automatic LS detection of pulmonary diseases. The advantage of SCMC is capturing the weighted average magnitude based on given sub-bands, and efficiently characterizing LS signals. In addition, Thomson multi-taper (TMT) method is introduced in this paper to replace original single-taper method using Hamming window for the SCMC feature extraction. We refer to the modified SCMC feature with TMT method as TMT-SCMC feature. Because of the ad-vantages of weighted average magnitude information and multi-taper method, the TMT-SCMC feature was expected to show significant differences between normal and pulmonary diseases signals, including normal versus asthma, normal versus pneumonia and normal versus chronic obstructive pulmonary disease (COPD). The contributions of this article can be summarized as follows: 1) To our best knowledge, the SCMC is first explored for LS detection of pulmonary diseases. Based on the optimal window length and suitable number of sub-bands, the experimental results showed that the SCMC is useful for the classification of normal versus pulmonary diseases.

Cover Page

DOI: http://ijmer.in.doi./2023/12.07.88
www.ijmer.in

INTERNATIONAL JOURNAL OF MULTIDISCIPLINARY EDUCATIONAL RESEARCH
ISSN:2277-7881; IMPACT FACTOR :8.017(2023); IC VALUE:5.16; ISI VALUE:2.286
Peer Reviewed and Refereed Journal: VOLUME:12, ISSUE:7(5), July: 2023
Online Copy of Article Publication Available (2023 Issues)
Scopus Review ID: A2B96D3ACF3FEA2A
Article Received: 2nd July 2023
Publication Date:30th July 2023
Publisher: Sucharitha Publication, India
Digital Certificate of Publication: www.ijmer.in/pdf/e-CertificateofPublication-IJMER.pdf

2. Proposed feature extraction

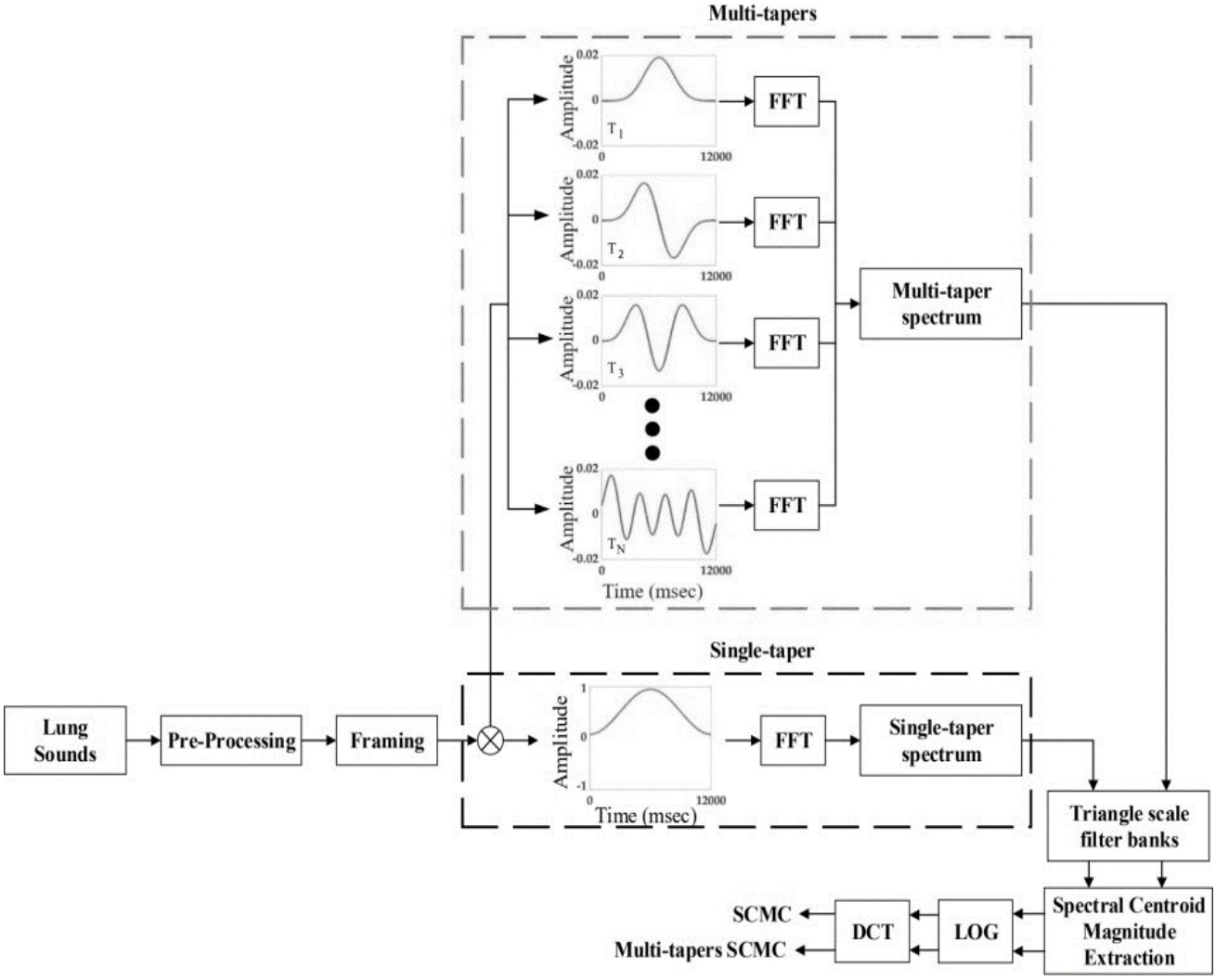

Figure 1. The block diagram of original SCMC and TMT-SCMC features extraction

2.1. Original SCMC extraction

SCMC was proposed by [23] for speaker recognition task. It can be calculated based on the Discrete Cosine Transform (DCT) of log spectral centroid magnitude of signal's sub-band spectral centroid magnitude information. The SCMC has properties similar to formant frequencies [23] that significantly characterize the acoustic scenes.
By following the same configuration with [12], the spectrum $S(f)$ of a LS signal is first computed by Fast Fourier Transform (FFT) of a LS frame, $x(t)$ in the time domain. Next, the discrete spectrum $S(f)$ is divided into M sub-bands using a series of triangle scale filter-banks where frequency responses denote $W_m(f)$. As suggested in [23,24], Spectral Centroid Magnitude, SCM ,is based on the weighted average magnitude spectrum in the sub-bands. It is calculated by averaging energy as given by:

Cover Page

INTERNATIONAL JOURNAL OF MULTIDISCIPLINARY EDUCATIONAL RESEARCH
ISSN:2277-7881; IMPACT FACTOR :8.017(2023); IC VALUE:5.16; ISI VALUE:2.286
Peer Reviewed and Refereed Journal: VOLUME:12, ISSUE:7(5), July: 2023
Online Copy of Article Publication Available (2023 Issues)
Scopus Review ID: A2B96D3ACF3FEA2A
Article Received: 2nd July 2023
Publication Date:30th July 2023
Publisher: Sucharitha Publication, India
Digital Certificate of Publication: www.ijmer.in/pdf/e-CertificateofPublication-IJMER.pdf

DOI: http://ijmer.in.doi./2023/12.07.88
www.ijmer.in

$$SCM_m = \frac{\sum_{f=lm}^{Um} f\,|W_m(f)S(f)|}{\sum_{f=lm}^{Um} f}, \; m = 1,2,3,...,M \qquad (1)$$

To reduce the dynamic range and decorrelate the features, the DCT is applied to the log of the SCM vector to obtain the final SCMC feature vector as follows

$$SCMC_l = \frac{1}{M}\sum_{m=1}^{M}|\log(SCM_m)|\cos\left(\frac{l\pi(m+0.5)}{M}\right), \quad l = 1, 2, 3,..., N_C \qquad (2)$$

where l denotes the number of cepstral coefficients and N_C is the number of the SCMC representation. Further details of the SCMC feature extraction can be seen in [18,25]. The process of SCMC feature extraction is shown in Figure 1

2.2. TMT-SCMC extraction

From the previous subsection, the original SCMC features are usually calculated from a Hamming-windowed periodogram spectrum estimate as follows

$$S(f) = \left|\sum_{t=1}^{N} w(t)s(t)e^{-i2\pi tf/N}\right| \qquad (3)$$

where $f \in \{1, 2, 3,..., N\}$ represents the discretefrequency index and $w \in [w(1), w(2), w(3),..., w(N)]$ is the time-domain window function.

Although the extraction of a single spectrum using a single-taper method and a Hamming window can provide detailed information, the spectrum representation still has a high variance estimation and may not be sufficient to characterize diseases from LS signals. To overcome this problem, previous works in the field of speaker verification tasks suggested that average spectral estimate using a set of different tapers could reduce large variance spectrum when compared with single-taper method. Motivated by speaker verification task, which is one type of audio classification, multi-taper method is introduced to replace the single taper methods for obtaining multi-taper spectrum estimate, $S(f)$. It is obtained by

$$S_{mt}(f) = \sum_{j=1}^{N_{mt}} \lambda(j)\left|\sum_{t=1}^{N} w_j(t)x(t)e^{-i2\pi tf/N}\right| \qquad (4)$$

where w_j is the j^{th} data taper 1,2,3, , N_{mt} (which are used with corresponding weights, $\lambda(j)$).

In this paper, TMT method is used to perform multi-taper spectrum estimation. It is specified from the Slepian sequences. Slepian sequences is based on unit-energy sequences on [0, S]. Slepian tapers is applied to overcome eigenvalue problem as follows:

$$Aw_j^p = v_j w_j^n \qquad (5)$$

Cover Page

INTERNATIONAL JOURNAL OF MULTIDISCIPLINARY EDUCATIONAL RESEARCH
ISSN:2277-7881; IMPACT FACTOR :8.017(2023); IC VALUE:5.16; ISI VALUE:2.286
Peer Reviewed and Refereed Journal: VOLUME:12, ISSUE:7(5), July: 2023
Online Copy of Article Publication Available (2023 Issues)
Scopus Review ID: A2B96D3ACF3FEA2A
Article Received: 2nd July 2023
Publication Date:30th July 2023
Publisher: Sucharitha Publication, India
Digital Certificate of Publication: www.ijmer.in/pdf/e-CertificateofPublication-IJMER.pdf

DOI: http://ijmer.in.doi./2023/12.07.88
www.ijmer.in

where $0 \leq p \leq S$, and $0 \leq n \leq S$, v_j denote the eigen-values ranging from zero to unity where $0 \leq v_j \leq 1$. A represents a real symmetric Toeplitz matrix with each element derived from

$$a_{nj} = \frac{\sin 2\pi B(n-p)}{\pi(n-p)}$$

where B is the half-frequency bandwidth.

3. Experimental Setup

3.1 Lung Sound Database

In this paper, a public database [16] is used to investigate the performance of the proposed feature for LS detection of pulmonary diseases. The database was a record of 35 healthy (normal) and 77 unhealthy (unnormal) subjects with the age averaged at 50.5 years. All recorded LS signals were sampled at 4000 Hz. The abnormal LS signals were produced from subjects with asthma, pneumonia, COPD, heart failure, lung fibrosis, and pleural effusion pathologies. The LS recordings for asthma, COPDs, pneumonia, and normal classes were used for our studies. The current experiments employed 105, 96, 27, and 15 LS signals to investigate the performance of our proposed feature for normal, asthma, COPDs, pneumonia classes, respectively.

3.2 Feature extraction

Since it is important to minimize heart sounds and noise effects, two methods were implemented. The 12th order Butterworth band-pass filter method with 120-1800 Hz was applied on raw LS signal as suggested in [17,26] for the pre-processing. Then, the filtered signal w further denoised using the 8th order Daubechies db14 Wavelet method summarized in [25]. For framing operation, the signals were divided using a fixed frame size of 3s with 50 % overlap between LS frames, which gave the best detection performance. In addition, different frame lengths of 20ms,240ms, 250ms, 256ms, 500ms, and 1s, 2s with 50% overlap and 4s, 5s with non-overlap were investigated but they did not improve the accuracy. These results meant that the frame length of 3 s with 50 % overlap between LS frames was more suitable for the original and our proposed SCMC features. Triangle scale filter-bank was used for the sub-band calculation as suggested in [24]. In this paper, we modified the publicly available pro-gram code provided by [24] to calculate the SCMC and TMT-SCMC feature. The next section analyzes the optimal number of sub-bands for maximum effective accuracy in SCMC and the optimal minimum taper for maximum effective accuracy in TMT-SCMC. For the feature extraction of SCMC method, TMT method was exploited to achieve promising performance. However, the results of using sine-weighted cestrum estimator and multipeak methods, which are not reported here, demonstrate no significant performance difference. This suggests that TMT method is particularly suitable to achieve high detection performance. In this paper, as suggested in [24], the original SCMC and TMT-SCMC were concatenated with their delta and delta-delta coefficients.

3.3 Classifiers

Because it can distinguish between data from different classes by determining an optimal hyperplane with the largest possible margin (the detailed procedure on the SVM classifier can be found in [5,12]), SVM has drawn a lot of attention in terms of LS detection of pulmonary diseases. Recent works [5,9,11-14] have reported that the SVM-

Cover Page

DOI: http://ijmer.in.doi./2023/12.07.88
www.ijmer.in

INTERNATIONAL JOURNAL OF MULTIDISCIPLINARY EDUCATIONAL RESEARCH
ISSN:2277-7881; IMPACT FACTOR :8.017(2023); IC VALUE:5.16; ISI VALUE:2.286
Peer Reviewed and Refereed Journal: VOLUME:12, ISSUE:7(5), July: 2023
Online Copy of Article Publication Available (2023 Issues)
Scopus Review ID: A2B96D3ACF3FEA2A
Article Received: 2nd July 2023
Publication Date:30th July 2023
Publisher: Sucharitha Publication, India
Digital Certificate of Publication: www.ijmer.in/pdf/e-CertificateofPublication-IJMER.pdf

based classifier demonstrates promising results for LS detection of pulmonary diseases. In this paper, we employed SVM as the detector in our experiment. Here, the publicly available Scikit-learn (Sklearn) libraries was used to train all the classifier models. For SVM, the penalty parameter C was set to 1, the kernel function was radial basis function, and the rest parameters were the default values.

3.4 Evaluation criteria

In this paper, we followed the evaluation setup explained in [10]. The 5-fold cross-validation is used to evaluate the overall classifier models and each of 5s duration signals, which were obtained by dividing LS recordings with a nonoverlapping duration, was considered for the experiment. Here, the numbers of 5s duration signals investigated normal, asthma, COPD, and pneumonia classes were obtained as 418, 366, 111, 63, respectively. The decision of the tested LS signals was based on the average score for all belonging segments. In this paper, the efficiency of our proposed feature was investigated for the detection of two classes (normal versus asthma/pneumonia/COPD) based on three common evaluations as follows

$$Sensitivity = \frac{TP}{TP + FN} \quad (6)$$

$$Specificity = \frac{TN}{(TN + FP)} \quad (7)$$

$$Accuracy = \frac{TP + TN}{TP + FN + TN + FP} \quad (8)$$

where TP and TN denote true pulmonary diseases and normal signals where the classifier correctly predicted abnormal and normal classes. FP and FN denote true pulmonary diseases and normal signals where the classifier incorrectly predicted ab-normal and normal classes. For the classifier with three classes (normal versus pneumonia versus asthma versus COPD), the efficiency of our proposed and applied feature was evaluated using accuracy as follows:

$$Ac_{AST} = \frac{Number\ of\ correctly\ classified\ asthma\ signals}{Total\ number\ of\ asthma\ signals\ under\ test} \quad (9)$$

$$Ac_{NOR} = \frac{Number\ of\ correctly\ classified\ normal\ signals}{Total\ number\ of\ normal\ signals\ under\ test} \quad (10)$$

$$Ac_{PNE} = \frac{Number\ of\ correctly\ classified\ pneumonia\ signals}{Total\ number\ of\ pneumonia\ signals\ under\ test} \quad (11)$$

4. Results and Discussion

4.1 Results based on binary detection

This section presents the detection performance of original SCMC and our pro-posed TMT- SCMC features. Because the number of sub-bands affect the effectiveness of SCMC feature, we first found out the optimal number of sub-bands

Cover Page

INTERNATIONAL JOURNAL OF MULTIDISCIPLINARY EDUCATIONAL RESEARCH
ISSN:2277-7881; IMPACT FACTOR :8.017(2023); IC VALUE:5.16; ISI VALUE:2.286
Peer Reviewed and Refereed Journal: VOLUME:12, ISSUE:7(5), July: 2023
Online Copy of Article Publication Available (2023 Issues)
Scopus Review ID: A2B96D3ACF3FEA2A
Article Received: 2nd July 2023
Publication Date:30th July 2023
Publisher: Sucharitha Publication, India
Digital Certificate of Publication: www.ijmer.in/pdf/e-CertificateofPublication-IJMER.pdf

DOI: http://ijmer.in.doi./2023/12.07.88
www.ijmer.in

for automatic LS detection of pulmonary diseases in order to obtain the highest accuracy. Figure 2 demonstrates the performance of SCMC using various number of sub-bands ranging from 20 to 200 by the step size of 20. It is clear that increasing the number of sub-bands from 20 to 160 led to an improvement in average accuracy, but using more than 160 sub-bands had no further effect on average accuracy. These outcomes indicate that the SCMC using standard sub-bands (20 sub-bands or 40 sub-bands) based on speech classification applications was insufficient to capture LS - relevant and the SCMC based on 160 sub-bands (optimal sub-bands for LS detection) provided the best performance with the average accuracy of 95.59 %. As a result, the SCMC based on 160 sub-bands was used as baseline SCMC feature with single taper method and compared with other features.

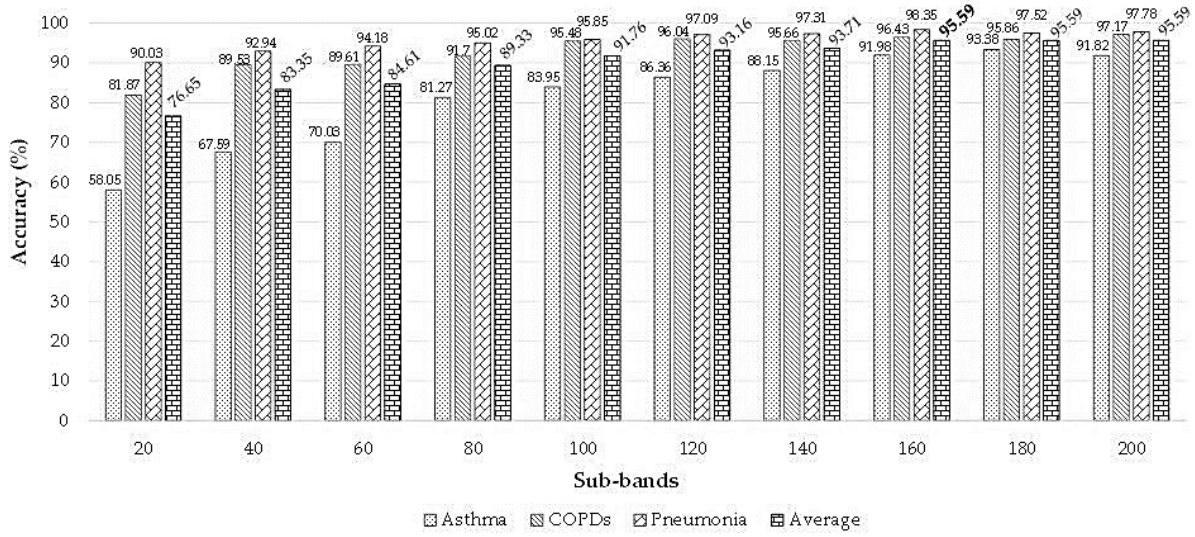

Figure 2. Accuracy of SCMC based on different sub-bands.

Next, we analyzed the effectiveness of TMT-SCMC feature using different tapers. Figure 3 demonstrates the performance of TMT-SCMC using several tapers. Figure 3 shows that the TMT method was very helpful for improving the original SCMC feature performance for lung disease LS detection because the feature extraction from multi-taper spectrum could provide information on how to distinguish between a normal and abnormal LS signal. Additionally, it can be seen that the TMT- SCMC with 260 tapers could achieve an average accuracy of 100% for the LS detection for normal versus asthma, normal versus pneumonia, and normal versus COPD. These results confirmed that TMT-SCMC was powerful for pulmonary disease verification from LS signals.

Finally, various numbers of tapers were varied from 242 tapers to 248 tapers by the step size of 2 tapers to investigate the maximum detection performance with the minimum number of tapers as shown in Figure 4. It can be seen that TMT-SCMC using 256 tapers provided the same performance as the TMT-SCMC using more than 256 tapers. This indicates that TMT-SCMC using 256 tapers was still efficient and it provided faster computation time due to minimum tapers. Here, TMT-SCMC feature based on 160 sub-bands and 256 tapers was used to compare other feature extraction methods.

Cover Page

DOI: http://ijmer.in.doi./2023/12.07.88
www.ijmer.in

INTERNATIONAL JOURNAL OF MULTIDISCIPLINARY EDUCATIONAL RESEARCH
ISSN:2277-7881; IMPACT FACTOR :8.017(2023); IC VALUE:5.16; ISI VALUE:2.286
Peer Reviewed and Refereed Journal: VOLUME:12, ISSUE:7(5), July: 2023
Online Copy of Article Publication Available (2023 Issues)
Scopus Review ID: A2B96D3ACF3FEA2A
Article Received: 2nd July 2023
Publication Date:30th July 2023
Publisher: Sucharitha Publication, India
Digital Certificate of Publication: www.ijmer.in/pdf/e-CertificateofPublication-IJMER.pdf

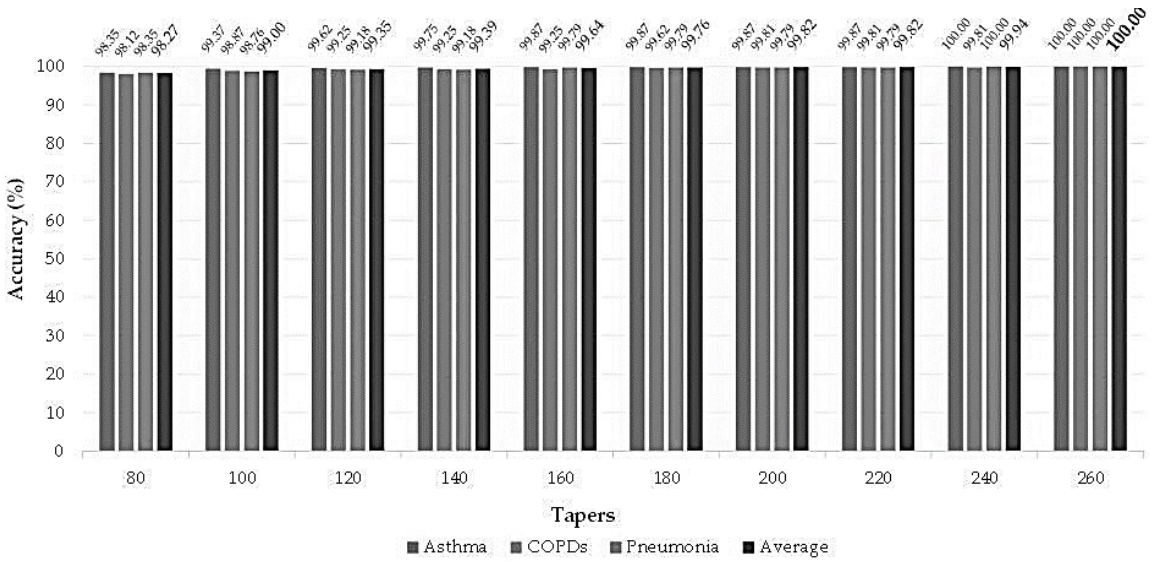

Figure 3. The accuracy of TMT-SCMC feature based on different tapers sub-bands varied from 80 to 260 by the step size of 20.

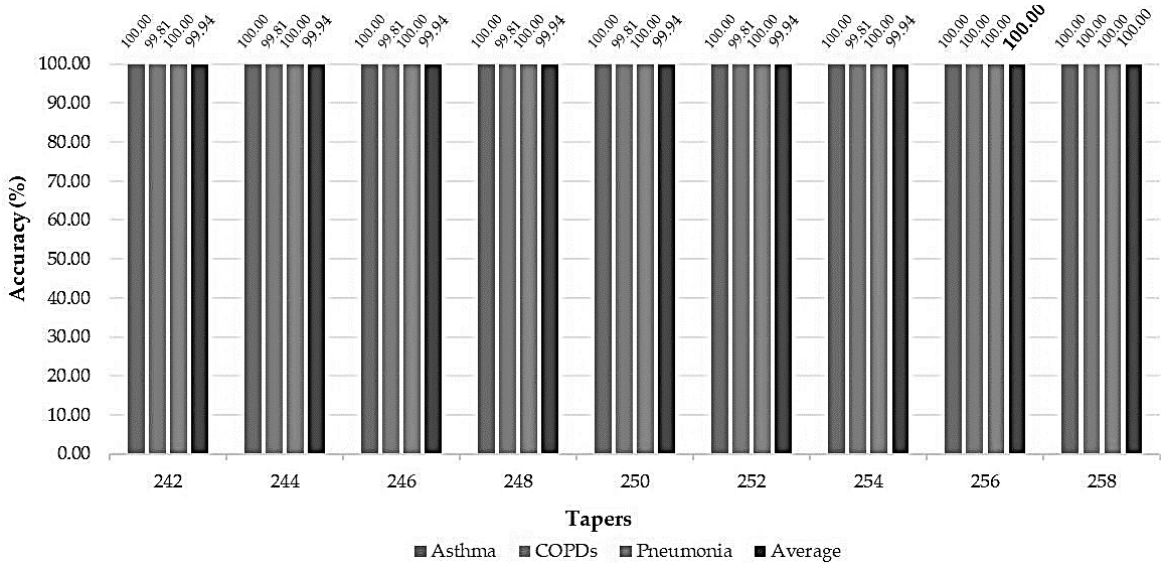

Figure 4. The accuracy of TMT-SCMC feature based on different tapers sub-bands varied from 242 to 248 by the step size of 2.

Cover Page

INTERNATIONAL JOURNAL OF MULTIDISCIPLINARY EDUCATIONAL RESEARCH
ISSN:2277-7881; IMPACT FACTOR :8.017(2023); IC VALUE:5.16; ISI VALUE:2.286
Peer Reviewed and Refereed Journal: VOLUME:12, ISSUE:7(5), July: 2023
Online Copy of Article Publication Available (2023 Issues)
Scopus Review ID: A2B96D3ACF3FEA2A
Article Received: 2nd July 2023
Publication Date:30th July 2023
Publisher: Sucharitha Publication, India
Digital Certificate of Publication: www.ijmer.in/pdf/e-CertificateofPublication-IJMER.pdf

DOI: http://ijmer.in.doi./2023/12.07.88
www.ijmer.in

4.2 Results based on the classification of three classes

This subsection reports the classification performance with three classes. Table 1 shows the results of the classification with three classes using the SCMC and muti-taper SCMC feature. The comparison between the original SCMC and TMT-SCMC showed that multi-taper outperformed the original SCMC feature because multi-taper method could efficiently average spectrum making TMT- SCMC robust to variance representation. A similar tendency was observed in the binary detection mentioned in previous subsection. These results suggested that TMT-SCMC feature is useful for the classification of three classes for automatic LS detection of pulmonary diseases.

Table 1. Performances of the classification of three classes based on SCMC and TMT-SCMC features.

Feature extraction	AC_{NOR}	AC_{PNE}	AC_{AST}	***OA(%)***
SCMC	88.47	89.23	93.74	90.48
TMT-SCMC	100.00	100.00	98.63	99.40

4.4 Comparison with other methods

This subsection presents the performance of the proposed feature compared with those of some known systems referred in [10]. From the introduction section, some systems were not comparable with our proposed SCMC features due to different databases. Tables 2 and 3 report the results of some known systems compared with the proposed SCMC feature methods for the classification of two and three classes, respectively.

Table 2. Comparison with other methods based on two classes.

Classification Scheme (results reported in [10])	**Features**	**Classifiers**	**Accuracy**	**Sensitivity**	**Specificity**
Normal versus Asthma	EWT	KNN	48.14 ± 3.45	80.11 ± 4.70	37.37 ± 5.53
	EWT	MLP	48.14 ± 3.45	33.60 ± 47.20	64.71 ± 48.32
	EWT	SVM	64.19 ± 4.23	67.97 ± 6.02	59.89 ± 4.57
	EWT	RF	77.08 ± 2.99	87.68 ± 3.16	65.08 ± 4.42
	EWT	XGboost	73.39 ± 3.21	77.73 ± 3.63	68.47 ± 4.34
	EWT	LGBN	80.35 ± 3.78	84.88 ± 4.21	75.23 ± 3.49
	SCMC	SVM	91.98 ± 4.73	88.76 ± 5.02	95.65 ± 5.52
	TMT- SCMC	SVM	100.00 ± 0.00	100.00 ± 0.00	100.00 ± 0.00

Cover Page

DOI: http://ijmer.in.doi./2023/12.07.88
www.ijmer.in

INTERNATIONAL JOURNAL OF MULTIDISCIPLINARY EDUCATIONAL RESEARCH
ISSN:2277-7881; IMPACT FACTOR :8.017(2023); IC VALUE:5.16; ISI VALUE:2.286
Peer Reviewed and Refereed Journal: VOLUME:12, ISSUE:7(5), July: 2023
Online Copy of Article Publication Available (2023 Issues)
Scopus Review ID: A2B96D3ACF3FEA2A
Article Received: 2nd July 2023
Publication Date:30th July 2023
Publisher: Sucharitha Publication, India
Digital Certificate of Publication: www.ijmer.in/pdf/e-CertificateofPublication-IJMER.pdf

Normal versus Pneumonia	EWT	KNN	74.42 ± 11.45	92.50 ± 3.53	100.00 ± 0.00
	EWT	MLP	74.42 ± 11.45	82.00 ± 20.57	60.00 ± 54.77
	EWT	SVM	100.00 ± 0.00	100.00 ± 0.00	100.00 ± 0.00
	EWT	RF	100.00 ± 0.00	100.00 ± 0.00	100.00 ± 0.00
	EWT	XGboost	99.01 ± 0.89	96.50 ± 2.85	100.00 ± 0.00
	EWT	LGBN	99.34 ± 0.89	99.00 ± 1.36	100.00 ± 0.00
	SCMC	SVM	98.35 ± 2.26	99.52 ± 1.06	90.77 ± 13.76
	TMT- SCMC	SVM	100.00 ± 0.00	100.00 ± 0.00	100.00 ± 0.00
Normal versus COPD	EWT	KNN	67.78 ± 4.88	90.50 ± 3.70	31.01 ± 9.03
	EWT	MLP	67.78 ± 4.88	90.00 ± 16.95	33.32 ± 30.46
	EWT	SVM	79.33 ± 2.22	86.59 ± 2.85	68.42 ± 8.64
	EWT	RF	77.50 ± 4.11	88.50 ± 3.35	60.39 ± 7.37
	EWT	XGboost	81.16 ± 7.28	87.00 ± 5.96	72.15 ± 10.87
	EWT	LGBN	83.27 ± 2.44	89.49 ± 6.51	72.24 ± 8.33
	SCMC	SVM	96.43 ± 4.64	98.81 ± 2.06	87.59 ± 15.63
	TMT- SCMC	SVM	100.00 ± 0.00	100.00 ± 0.00	100.00 ± 0.00

From Table 2, it can be noted that TMT-SCMC feature outperformed all known systems in terms of accuracy, sensitivity, and specificity for binary classification. This suggests that TMT-SCMC is powerful for normal versus asthma, normal versus chronic obstructive pulmonary diseases (COPDs) because it could capture LS-relevant information effectively, based on exploiting the weighted average magnitude derived from multi-taper spectrum information.

5. Conclusions and Future Work

In this paper, SCMC feature was first explored for automatic LS detection of pulmonary diseases. In addition, we modified the original SCMC feature extraction by using TMT method to replace single taper method based on Hamming windows. We referred to the modified SCMC feature as TMT-SCMC. The performances of the explored and

Cover Page

DOI: http://ijmer.in.doi./2023/12.07.88
www.ijmer.in

INTERNATIONAL JOURNAL OF MULTIDISCIPLINARY EDUCATIONAL RESEARCH
ISSN:2277-7881; IMPACT FACTOR :8.017(2023); IC VALUE:5.16; ISI VALUE:2.286
Peer Reviewed and Refereed Journal: VOLUME:12, ISSUE:7(5), July: 2023
Online Copy of Article Publication Available (2023 Issues)
Scopus Review ID: A2B96D3ACF3FEA2A
Article Received: 2nd July 2023
Publication Date:30th July 2023
Publisher: Sucharitha Publication, India
Digital Certificate of Publication: www.ijmer.in/pdf/e-CertificateofPublication-IJMER.pdf

our proposed features were investigated using the publicly available database with five-fold cross-validation. The experimental results demonstrated that the SCMC feature with 160 sub-bands was useful for automatic LS detection of pulmonary diseases based on 3s frame length with 50% overlap. The SCMC provided average accuracies of 91.98% for normal versus asthma, 98.35% for normal versus pneumonia, and 96.43% for normal versus COPD, 90.44% for normal versus asthma versus pneumonia. Moreover, the TMT-SCMC feature based on 160 sub-bands and 256 tapers pro-vided the average accuracies of 100.00% for normal versus asthma/pneumonia/COPD, 99.40 % for normal versus asthma versus pneumonia. These results suggested that TMT-SCMC was very powerful for the LS classification for discriminating pulmonary diseases from normal signals. In future work, we would like to combine relative phase information [28,29] with the proposed feature and attempt to investigate the proposed feature based on empirical mode decomposition method [30].

6.Competing interests

No conflict of interest exists. We wish to confirm that there are no known conflicts of interest associated with this publication and there has been no significant financial support for this work that could have influenced its outcome.

7.Funding

Not applicable

8.Authors' contributions

(a). Conception, acquisition of data and design of study, analysis and interpretation of data, and drafting of manuscript : all authors contributed
(b). Approval of the version of the manuscript to be published: all authors consent

References

1. ALTAN, G.; Kutlu, Y.; Garbi, Y.; Pekmezci, A. Ö.; Nural, S. (2017). Multimedia respiratory database (RespiratoryDatabase@ TR): Auscultation sounds and chest X-rays. Natural and Engineering Sciences, 2(3), 59-72.
2. Andrès, E.; Gass, R.; Charloux, A.; Brandt, C.; Hentzler, A. (2018). Respiratory sound analysis in the era of evidence-based medicine and the world of medicine 2.0. Journal of medicine and life, 11(2), 89.
3. Demir, F.; Sengur, A.; Bajaj, V. (2020). Convolutional neural networks based efficient approach for classification of lung diseases. Health information science and systems, 8(1),1-8.
4. Amrulloh, Y.; Abeyratne, U.; Swarnkar, V.; Triasih, R. (2015). Cough sound analysis for pneumonia and asthma classification in pe-diatric population. In 2015 6th International Conference on Intelligent Systems, February, Modelling and Simulation, pp. 127-131.
5. Abbasi, S.; Derakhshanfar, R.; Abbasi, A.; Sarbaz, Y. (2013). Classification of normal and abnormal lung sounds using neural network and support vector machines. In 2013 21st Iranian Conference on Electrical Engineering (ICEE), May, pp. 1-4.
6. Uysal, S.; Uysal, H.; Bolat, B.; Yıldırım, T. (2014). Classification of normal and abnormal lung sounds using wavelet coefficients. In 2014 22nd Signal Processing and Communications Applications Conference (SIU), April, pp. 2138-2141.
7. Liu, Y.; Zhang, C. M.; Zhao, Y. H.; Dong, L. (2006). The feature extraction and classification of lung sounds based on wavelet packet multiscale analysis. Chinese Journal of Computers, 29(5), 769.
8. Sengupta, N.; Sahidullah, M.; Saha, G. (2016). Lung sound classification using cepstral-based statistical features. Computers in biol-ogy and medicine, 75, 118-129.


Cover Page

INTERNATIONAL JOURNAL OF MULTIDISCIPLINARY EDUCATIONAL RESEARCH
ISSN:2277-7881; IMPACT FACTOR :8.017(2023); IC VALUE:5.16; ISI VALUE:2.286
Peer Reviewed and Refereed Journal: VOLUME:12, ISSUE:7(5), July: 2023
Online Copy of Article Publication Available (2023 Issues)
Scopus Review ID: A2B96D3ACF3FEA2A
Article Received: 2nd July 2023
Publication Date:30th July 2023
Publisher: Sucharitha Publication, India
Digital Certificate of Publication: www.ijmer.in/pdf/e-CertificateofPublication-IJMER.pdf

DOI: http://ijmer.in.doi./2023/12.07.88
www.ijmer.in

9. Azmy, M. M. (2015). Classification of lung sounds based on linear prediction cepstral coefficients and support vector machine. In 2015 IEEE Jordan Conference on Applied Electrical Engineering and Computing Technologies (AEECT), November, pp. 1-5.
10. Tripathy, R. K.; Dash, S.; Rath, A.; Panda, G.; Pachori, R. B. (2022). Automated Detection of Pulmonary Diseases from Lung Sound Signals Using Fixed-Boundary-Based Empirical Wavelet Transform. IEEE Sensors Letters, 6(5), 1-4.
11. Emmanouilidou, D.; McCollum, E. D.; Park, D. E.; Elhilali, M. (2017). Computerized lung sound screening for pediatric auscultation in noisy field environments. IEEE Transactions on Biomedical Engineering, 65(7), 1564-1574.
12. Palaniappan, R.; Sundaraj, K.; Sundaraj, S. (2014) A comparative study of the svm and k-nn machine learning algorithms for the diagnosis of respiratory pathologies using pulmonary acoustic signals. BMC bioinformatics, 15(1), 1-8.
13. Islam, M. A.; Bandyopadhyaya, I.; Bhattacharyya, P.; Saha, G. (2018). Multichannel lung sound analysis for asthma detection. Com-puter methods and programs in biomedicine, 159, 111-123.
14. Fraiwan, L.; Hassanin, O.; Fraiwan, M.; Khassawneh, B.; Ibnian, A. M.; Alkhodari, M. (2021). Automatic identification of respiratory diseases from stethoscopic lung sound signals using ensemble classifiers. Biocybernetics and Biomedical Engineering, 41(1), 1-14.
15. Haider, A.; Ashraf, M. D.; Azhar, M. U.; Maruf, S. O.; Naqvi, M.; Khawaja, S. G.; Akram, M. U. (2014). Separation and classification of crackles and bronchial breath sounds from normal breath sounds using Gaussian mixture model. In International Conference on Neural Information Processing, Springer, Cham, November, pp. 495-502.
16. Bardou, D.; Zhang, K.; Ahmad, S. M. (2018). Lung sounds classification using convolutional neural networks. Artificial intelligence in medicine, 88, 58-69.
17. Serbes, G.; Ulukaya, S.; Kahya, Y. P. (2017). An automated lung sound preprocessing and classification system based onspectral analysis methods. In International Conference on Biomedical and Health Informatics, Springer, Singapore, November, pp. 45-49.
18. Kinnunen, T.; Saeidi, R.; Sedlák, F.; Lee, K. A.; Sandberg, J.; Hansson-Sandsten, M.; Li, H. (2012). Low variance multitaper MFCC features: a case study in robust speaker verification. IEEE transactions on audio, speech, and language processing, 20(7), 1990-2001.
19. Sandberg, J.; Hansson-Sandsten, M.; Kinnunen, T.; Saeidi, R.; Flandrin, P.; Borgnat, P. (2010). Multitaper estimation of frequency-warped cepstra with application to speaker verification. IEEE Signal Processing Letters, 17(4), 343-346.
20. Gunendradasan, T.; Wickramasinghe, B.; Le, P. N.; Ambikairajah, E.; Epps, J. (2018). Detection of Replay-Spoofing Attacks Using Frequency Modulation Features. In Interspeech, September, pp. 636- 640.
21. Le, P. N.; Ambikairajah, E.; Epps, J.; Sethu, V.; Choi, E. H. (2011). Investigation of spectral centroid features for cognitive load classi-fication. Speech Communication, 53(4), 540-551.
22. Chapaneri, S. V.; Jayaswal, D. D. (2015). Multi-taper spectral features for emotion recognition from speech. In 2015 International Conference on Industrial Instrumentation and Control (ICIC), May, pp. 1044-1049.
23. Kua, J. M. K.; Thiruvaran, T.; Nosratighods, M.; Ambikairajah, E.; Epps, J. (2010). Investigation of spectral centroid magnitude and frequency for speaker recognition. In Odyssey, June, p. 7.
24. Sahidullah, M.; Kinnunen, T.; Hanilçi, C. (2015). A comparison of features for synthetic speech detection. Interspeech, September 6-10, 2015, Dresden, Germany.
25. Alam, M. J.; Kinnunen, T.; Kenny, P.; Ouellet, P.; O'Shaughnessy, D. (2013). Multitaper MFCC and PLP features for speaker verification using i-vectors. Speech communication, 55(2), 237-251.
26. Minami, K.; Lu, H.; Kim, H.; Mabu, S.; Hirano, Y.; Kido, S. (2019). Automatic classification of largescale respiratory sound dataset based on convolutional neural network. In 2019 19th International Conference on Control, Automation and Systems (ICCAS), October, pp. 804-807.
27. Hinton, G.; van der Maaten, L. (2008). Visualizing data using t-SNE. Journal of Machine Learning Research.
28. Phapatanaburi, K.; Pathonsuwan, W.; Wang, L.; Anchuen, P.; Jumphoo, T.; Buayai, P.; Uthansakul, P. (2022). Whispered Speech De-tection Using Glottal Flow-Based Features. Symmetry, 14(4), 777.


Cover Page

INTERNATIONAL JOURNAL OF MULTIDISCIPLINARY EDUCATIONAL RESEARCH
ISSN:2277-7881; IMPACT FACTOR :8.017(2023); IC VALUE:5.16; ISI VALUE:2.286
Peer Reviewed and Refereed Journal: VOLUME:12, ISSUE:7(5), July: 2023
Online Copy of Article Publication Available (2023 Issues)
Scopus Review ID: A2B96D3ACF3FEA2A
Article Received: 2nd July 2023
Publication Date:30th July 2023
Publisher: Sucharitha Publication, India
Digital Certificate of Publication: www.ijmer.in/pdf/e-CertificateofPublication-IJMER.pdf

DOI: http://ijmer.in.doi./2023/12.07.88
www.ijmer.in

29. Phapatanaburi, K.; Wang, L.; Nakagawa, S.; Iwahashi, M. (2019). Replay attack detection using linear prediction analysis-based rela-tive phase features. IEEE Access, 7, 183614-183625.
30. Dar J.A., Srivastava K.K., Ahmed Lone S.(2022).Design and development of hybrid optimization enabled deep learning model for COVID-19 detection with comparative analysis with DCNN, BIAT-GRU,XGBoost Computers in Biology and Medicine, 150 , art. no. 106123.
31. Phapatanaburi, K.; Kokkhunthod, K.; Wang, L.; Jumphoo, T.; Uthansakul, M.; Boonmahitthisud, A.; Uthansakul, P. (2021). Brainwave classification for character-writing application using emd-based GMM and KELM approaches. CMC-Computers, Materials & Continua, 66(3), 3029-3044.

ISSN: 0976-3031

Available Online at http://www.recentscientific.com

CODEN: IJRSFP (USA)

International Journal of Recent Scientific Research
Vol. 14, Issue, 08 (A), pp. xxx-xxx, August, 2023

International Journal of Recent Scientific Research

DOI: 10.24327/IJRSR

Research Article

ANALYSIS OF DIFFERENT COGNITIVE ACTIVITIES (REST, MEDITATION, AND ARITHMETIC), AND THEIR ALPHA AND THETA BAND FREQUENCIES

Atanu Manna[1] and Kamal Kr. Srivastava[2]

[1,2]Department of Computer Science and Engineering, Mansarovar Global University Madhya Pradesh India

DOI: http://dx.doi.org/10.24327/ijrsr.2023.1408.0751

ARTICLE INFO

Article History:

xxxx

Keywords:

Cognitive task, mindfulness meditation, Electroencephalography, alpha-theta correlation, independent component analysis

ABSTRACT

Indication is presented that EEG fluctuations in the alpha and theta band reflect cognitive and memory performance in particular. Good recital is related to two types of EEG phenomena (i) a stimulant increase in alpha but a decrease in theta power, and (ii) a large phasic (event-related) decrease in alpha but increase in theta, depending on the type of memory demands. Because alpha frequency shows large interindividual differences which are related to age and memory performance, this double dissociation between alpha vs. theta and tonic vs. phasic changes can be observed only if fixed frequency bands are abandoned. It is suggested to adjust the frequency windows of alpha and theta for each subject by using individual alpha frequency as an anchor point. Based on this procedure, a consistent interpretation of a variety of findings is made possible. Brain oscillations vary due to neurological activities that play an important role in designing a cognitive task. In the proposed study, 27 subjects experimented with different cognitive activities (rest, meditation, and arithmetic), and their alpha and theta band frequencies were analyzed. BIOPAC-MP-160 has performed the data acquisition and further processing of the acquired dataset was performed in EEGLAB. The results illustrated that the cross-frequency correlation (alpha: theta: 1:2) between alpha and theta waves has been enhanced during effortful cognition. The alpha-theta cross-frequencies were observed to be maximum in the arithmetic state, while it remains low in both the resting and meditation states. Maximum episodes of the cross-frequency correlations occurred when alpha band frequencies lie between 9-12 Hz. The study also reveals that maximum alpha-theta cross-frequency (40.74%) was found at the electrode positions Af3 and Af4. The comparisons based on event-related potentials (ERPs) and power spectral densities (PSDs) have shown that the meditation state is more sluggish than the arithmetic and rest states.

INTRODUCTION

In a physiological sense, EEG power reflects the number of neurons that discharge synchronously. Because brain volume and the thickness of the cortical layer is positively correlated with intelligence, it is tempting to assume that EEG power too, is a measure that reflects the capacity or performance of cortical information processing. Although it will be argued that this is in principle the case, it must be emphasized that power measurements are strongly affected by a variety of unspecific factors such as the thickness of the skull or the volume of cerebrospinal fluid, by methodological and technical factors (such as interelectrode distance or type of montage) but also by more specific factors such as age, arousal and the type of cognitive demands during actual task performance.

In today's fast-paced world, it has been observed that very few people have time to focus on mindfulness meditation [1]. The primary goal of meditation is to control our thoughts with a focus on a specific object, such as focusing on the expanse, counting the breath, guided meditation, etc. [2, 3]. Along with the dissolution of the ego, detachment, and non-involvement with things have complimented meditation [4]. One of the goals of mindfulness meditation is to release one's brain from external interruptions, control one's thoughts, and In a physiological sense, EEG power reflects the number of neurons that discharge synchronously. Because brain volume and the thickness of the cortical layer is positively correlated with intelligence, it is tempting to assume that EEG power too, is a measure that reflects the capacity or performance of cortical information processing. Although it will be argued that this is in principle the case, it must be emphasized that power measurements are strongly affected by a variety of unspecific factors such as the thickness of the skull or the volume of cerebrospinal fluid, by methodological and technical factors (such as interelectrode distance or type of montage) but also by

Corresponding author:* **Atanu Manna
Department of Computer Science and Engineering, Mansarovar Global University Madhya Pradesh India

more specific factors such as age, arousal and the type of cognitive demands during actual task performance.

In today's fast-paced world, it has been observed that very few people have time to focus on mindfulness meditation [1]. The primary goal of meditation is to control our thoughts with a focus on a specific object, such as focusing on the expanse, counting the breath, guided meditation, etc. [2, 3]. Along with the dissolution of the ego, detachment, and non-involvement with things have complimented meditation [4]. One of the goals of mindfulness meditation is to release one's brain from lower the thought circle frequency to achieve a state of mental emptiness. The retrieval and manipulation of information during any designed cognitive task were seen as the essential function of the human brain that can be associated with the alpha (8-14 Hz) and theta (4-8 Hz) frequency bands [5-7]. Human brain efficiency can be increased through meditation and a relaxed mind, enabling better coordination in our daily tasks and leading a happy and healthy life [8, 9]. In recent years, ubiquitous and pervasive healthcare devices have been widely used for low-computational human health prediction. Electroencephalography (EEG) has been used to analyze brain oscillations in various mental states and detect human brain activity or neurological disorders. Various other techniques, e.g., functional magnetic resonance imaging (fMRI), positron emission tomography (PET), magnetoencephalography (MEG), and optical imaging, are also available for data acquisition. EEG has been used more frequently than other available techniques due to its high temporal resolution, low cost, availability, and noninvasive nature [10]. The brain oscillations reflect the neural activities due to various actions or thoughts of the subject. EEG frequencies played a crucial role in analyzing different cognitive states, e.g., arithmetic, meditation, and rest [11, 12]. Alpha (8-14Hz) and theta (4-8Hz) frequency bands have played a significant role and were often used to analyze and differentiate various mental states and cognitive activities [13-15]. Information storage and retrieval have been associated with the alpha band, while the theta band has been incorporated with information manipulation [16, 17]. While performing various mental tasks, the changes in alpha and theta band frequencies were observed by differentiating their peak amplitudes and powers [18]. The literature confirmed that the alpha-peak frequency was accelerated during effortful cognitive tasks [19], and alpha-theta peaks appeared around its harmonic, i.e., alpha: theta: 2:1 [20]. Some results also reported that alpha and theta powers were enhanced during meditation compared to rest [21-24]. However, the results differ between experienced mediators and novice meditators [25]. The frequency variations also depended on different meditation techniques [26, 27]. The literature revealed that most of the studies used 19, 23, 36, and more number of electrodes covering the entire scalp surface during analysis [28]. Very few studies are available that focus on a particular area of the brain.

In the present work, experimental analysis has been performed with a pair of channels at six different positions associated with the frontal lobe (i.e., Fp1, Fp2, Af3, Af4, Af7, and Af8). The main focus of this research is the study and analysis of changes in brain activation due to cognitive tasks such as rest, meditation, and arithmetic. This study demonstrated how the cross-frequency correlations in the brain's frontal region vary under different task conditions. A cognitive task has been designed having three different states (rest, meditation, and arithmetic). Since meditation is non-quantitative, the person has been meditated by hearing the OM chant on a specific frequency (963 Hz). Human systems have seven chakras [29]. Resonance frequencies for each chakra have been reported differently, starting from 436 Hz - 963 Hz [30]. Different colors are assigned to all chakras [30]. The crown chakra is purple and vibrates at 963 Hz to the central part of the brain. Such healing therapy is responsible for relaxation, mindfulness, deep meditation, etc. [31]. The crown chakra can be awakened by resonating it with the specific frequency produced by a particular sound. In the yogic tradition, around 963 Hz represents the crown chakra frequency. For this reason, a 963 Hz OM chanting frequency was chosen to induce a powerful state of meditation. In EEGLAB, a study with 27 test subjects and three different task conditions (rest, meditation, and arithmetic) was created, and ERP and PSD comparisons were analyzed. The paper is as follows: Section two consists of materials and methods, experiment design, participants, data acquisition system, electrode placement, and data processing. Section three contains the result. While sections four and five consist of discussion and conclusion, respectively.

MATERIALS AND METHODS

The specifics of the experiment design are well explained in this section, along with the data acquisition system and the processing techniques.

Task Design: The task design was a crucial step. The authors designed a specific cognitive task based on some textbooks and research [32-34]. Working minds a Practitioner's Guide to Cognitive Task Analysis by Robert R Hoffman [35] and a handbook on Cognitive Task Design: Human Factors and Ergonomics by Hendrik H. [36] helped us to design the cognitive task. All the factors, conditions, advantages, and disadvantages from the literature above were considered to design the task. The designed cognitive task consists of three states, i.e., rest, meditation, and arithmetic. The study details are summarized in Table 1. 20 minutes of data was collected for each condition. At rest, the test subjects were asked to close their eyes, feel free and de-attach themselves from the outside world interrupts and let go of thoughts. In the induced meditation state, subjects must listen to an Om chant at a specific frequency (963 Hz) for 20 min with closed eyes. During the arithmetic state, subjects were asked to subtract five from 100, and if they reached zero or lost track, they had to start again from 100. To make the length of the different states comparable, 5 minutes of data were analyzed for each state.

Table 1 Cognitive task states

Condition	Preparation	Delay in task
Rest	Made for relaxing for 20 minutes (eyes closed)	Ten minutes delay has been provided between the two different states of the task.
Meditation	Made to hear Om chanting (963Hz.) for 20 minutes(eyes closed)	
Arithmetic	Performed arithmetic operation for 20 minutes (eyes closed)	

Participants: 36 subjects volunteered to complete the study. Out of 36 subjects, outliers were found in 9 subject data. Some did not focus on the task, while the electrode placement was incorrect in some cases. For this reason, 27 subjects (N=27, S.D.=2.18, Mean=30.81, Variance=4.77) were found suitable for the data acquisition process. From 27 test persons, 18 men and 9 women between the ages of 22-36 years. The advertisement was published in templates pasted within the university premises for this voluntary task. All the subjects were graduates; some were postgraduate and Ph.D. students.

Subjects signed a consent form where they mentioned whether they have presently any physiological problem or faced it in the past, either taking any medication or suffering from any illness. Nobody was an alcoholic; one subject was left-handed out of 36 subjects. Before starting the data acquisition process, the subjects were asked how they feel, i.e., anxious, depressed, or normal. If the subject answered other than normal, the data acquisition process was postponed until the particular subject felt normal. Table 2 illustrates the demography of the subjects. The data was collected between November 2020 and January 2021. The data was collected on non-working days (Saturday and Sunday) from 4.00 p.m. to 7.00 p.m. IST at SLIET University.

Table 2 Subjects demography

Total no. of subjects	Gender/ Age	Education status	The present state of mind	Alcoholic	Any physiological problem	Any medication
27 (taken data of 36 subjects, 9 were found not suitable.	Out of 27 subjects,18M, nine F, age ranges between 22 to 36 years	Graduation, Masters's, and Ph.D. For better results, we chose only engineering graduates.	Depressed, stressed, or feeling normal.	None	None	One was diabetic type 2, so excluded from the data acquisition process.

Data Acquisition System & Electrode Placement

The data acquisition was completed using BIOPAC MP-160 with 27 university students for the designed task. Two channels of BIOPAC MP-160 were used for the EEG acquisition process. EEG Electrodes were placed according to the specific task requirements. The electrodes were placed according to the international 10-20 system [37], as shown in Figure 1. The size and shape of the test subject's heads were measured before attaching the electrodes. The scalp was measured individually by CADWELL tape, and electrodes were placed with the exact measurement of the dimensions of the individual scalp. Several calculations were carried out with each subject for six different frontal positions.

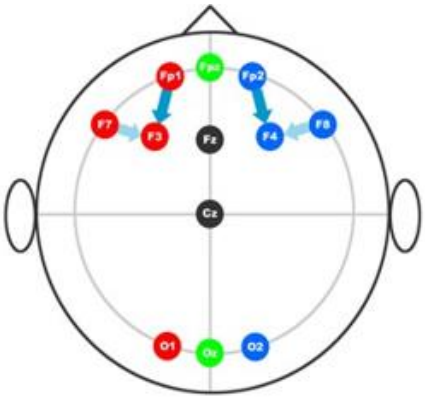

Figure 1 Electrode positions according to the international 10-20 system.

The placement of the electrodes was rechecked before starting the next measurement of the next condition if any of the connections shifted or loosened. First, the EEG electrodes were placed in Fp1 and Fp2 positions, and the task was carried out and the data recorded. The same pattern was repeated with Af3, Af4, and Af7, Af8 electrode positions. The surfaces were cleaned with a disinfectant to minimize the impedance between the electrode and the scalp. In most cases (i.e., most male subjects), it was relatively easy to place the electrodes in different positions, but in some cases (e.g., female subjects), the placement of the electrodes was difficult at Af3, Af4, Af7, Af8 positions due to the interference of hairs. All participants were asked to come with a cleansed scalp with a branded hair shampoo to reduce excess oil and dirt from the scalp. Therefore several attempts have been made to extract the data from these positions.

Processing of data: In this study, the features like ERP, SPD, and alpha-theta peaks were extracted and processed using EEGLAB. The three attained features have been compared in the three different states: rest, meditation, and arithmetic. The raw EEG data was loaded in EEGLAB, then re-sampled at 256 Hz, and basic filtering applied from 0.5 to 40 Hz, then decomposed in different frequency bands to analyze the task in these frequency bands. Artifacts are a common occurrence while recording the data. Hence they cannot be ignored.

The typical artifacts in the case of EEG signals may be differentiated into three categories: physiological, habitual, and external. In the physiological category, tingling, swallowing, twitching of muscle, and sweating artifacts were found in a few subjects.

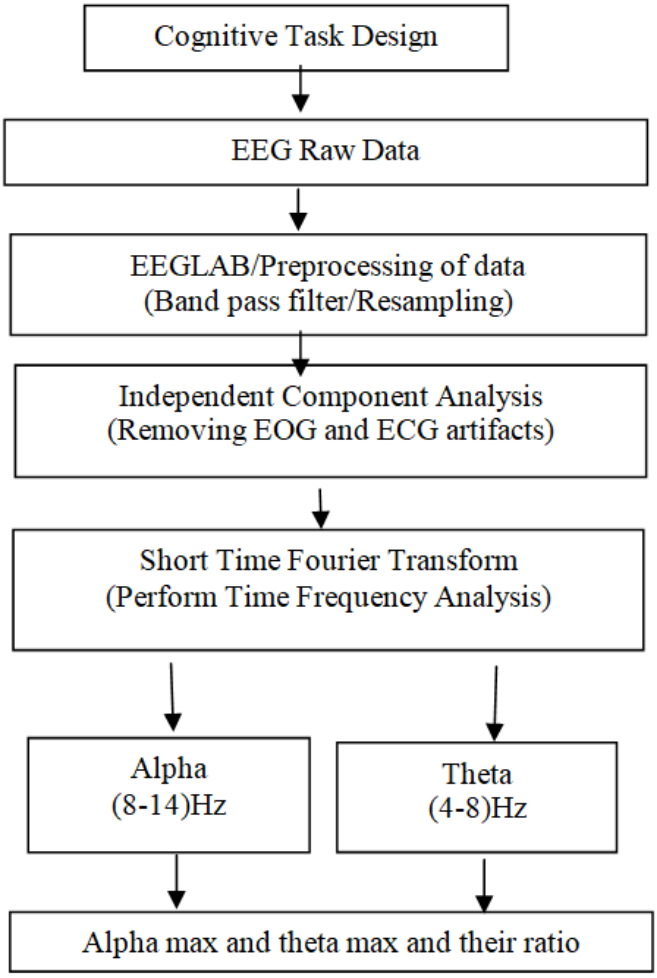

Figure 3 Flow chart of the methodology and signal processing

Whereas instructions were given to every subject to control physical activities during the task, but when observed closely, it was found that during the arithmetic condition, some subjects were not able to control their habitual behavior, i.e., counting

on fingers, frowning, feet movement, and too much movement of the eye and the tongue. Besides this, the power line interference was also considered the reason for the external artifacts. To minimize the artifacts, the subjects followed the standard instructions (i.e., not too much movement of eye or tongue, not talking and chewing, and not moving any body part during the task). Still, there were also interfering signals from alternating current power noise and fluorescent light. Such noises may result in erroneous brain wave measurement results or poor performance in brain-computer interfaces [38]. The eye-blinking artifacts, artifacts owing to heartbeats, and other noises have been removed by applying independent component analysis (ICA). ICA is a machine learning technique that separates independent sources from a mixed signal; it decomposes the composite signal into independent sources. Eye blinking signals primarily have a low frequency of less than 4 Hz, which affects the Fp1 and Fp2 channels, and they are the most interfering signal for EEG measurement because of their large amplitude. The frequency of EMG signals is typically considerably higher than that of brain waves, and these signals were mostly removed during EEG signal processing. Now the comparisons have been made based on the alpha and theta bands for the three different conditions of the cognitive task. After artifact rejection, short-time Fourier transform (STFT) was used to analyze the data in the frequency domain. Figure 3 illustrates the flow chart of the methodology. The instantaneous peak frequencies in the alpha (8-14Hz) and theta band (4-8 Hz) were detected for each 1-sec epoch of transformed data in MATLAB (version r2017b) using the local maxima functions, i.e., findpeaks [39], After finding the peak values of the ratio of alpha and theta peak frequencies have been calculated.

RESULT

This section discussed the alpha-theta correlations during the three different task conditions. Alpha-theta peak value-based comparisons and ERP, PSD-based analysis has been presented here.

Primarily Analysis (Alpha–Theta correlations during the task): After preprocessing and decomposition of data into alpha (8-14Hz) and theta (4-8Hz) frequencies, the computation of their peaks have been carried out for the different task states (rest, arithmetic and meditation). Table 3 summarized the approximate peak values of alpha and theta frequencies and their ratio at Fp1 and Fp2 electrodes positions. For example, when subject S0 was instructed to relax, the resting position alpha and theta frequencies calculated were 11.2 Hz and 6.2 Hz, respectively. During meditation, the alpha frequencies significantly decreased from 11.22 Hz to 9.71 Hz, and the theta frequency reduced from 6.2 Hz to 4.6 Hz. During the arithmetic task, the alpha frequency suddenly rises from 11.2 Hz to 13.6 Hz, and the theta frequency varies from 6.2 Hz to 7.7 Hz. It signifies that during the meditation state, the brain frequency decreases, while in any arithmetic state, the frequency increases for the subject S0. For the same subject, the alpha-theta cross-frequency ratio was approximately 1.8 Hz at rest, 2.1 Hz at meditation, and 1.7 Hz at arithmetic. Similarly, all 27 subjects have been analyzed, and it has been observed that during rest, the alpha-theta cross frequency (alpha:thera:2:1) occurs six times (i.e., for subjects S2, S3, and S10, S14, S18 and S26). In the meditation state, the alpha-theta cross-frequency occurrences have been found only twice (for subject S6 and S23), and in the arithmetic state, it happens nine times (for subjects S3, S5, S6, S11, S15, S17, S22, S23 and S26).
From these findings, it is clear that:

% of alpha-theta cross-frequency occurrences during arithmetic state= 9*100/27=33.33
% of alpha-theta cross-frequency occurrences during meditation state=2*100/27=7.40
% of alpha-theta cross-frequency occurrences during rest state= 6*100/27= 22.22

The above calculations show that the alpha-theta cross-frequency percentage value during arithmetic state (i.e., 33.33%) is far greater than the meditation state (i.e., 7.40%). Conversely, the alpha-theta cross-frequency percentage during the rest state (i.e., 22.22%) is greater than meditation State (i.e., 7.40%). The calculations made during the experiments comply with the cross-frequency occurrence pattern, i.e., arithmetic> rest>meditation.

The box plot of the dataset is shown in Figure 4. It can be observed that the mean values of meditation and rest state data were found less in comparison to the arithmetic state data. Whereas the width of the meditation box seems more than the remaining two boxes, which indicates the data range of the meditation state is more than the other two states. The outlier values have also been found in some states of the experiment. These outlier values may be caused due to some instantaneous distractions during the task or when the subject loses concentration and again immersed in the same task state. We had tried our best that every subject emerged fully with the task states, but no one can control all his thoughts for a given task within a given time.

Table 3 Peak frequencies values (Hz) values (approx.) of alpha, theta, and their ratios in three different task states, the electrodes were placed at Fp1, Fp2 position.

Sub	Rest			Meditation			Arithmetic		
	α(M)	θ(M	α/θ(M)	α(M)	θ(M)	α(M)/θ(M)	α(M)	θ(M)	α(M)/θ(M)
S0	11.2	6.2	1.8	9.7	4.6	2.1	13.6	7.7	1.7
S1	10.9	6.8	1.6	8.6	4.5	1.9	11.7	5.3	2.1
S2	9.3	4.6	2.0	7.3	4.5	1.6	12.1	6.3	1.9
S3	11.3	5.6	2.0	7.9	4.6	1.7	13.3	6.6	2.0
S4	10.7	6.5	1.6	8.3	5.2	1.6	12.3	5.9	2.1
S5	9.7	7.5	1.3	9.0	5.2	1.7	11.7	5.8	2.0
S6	13.1	7.3	1.8	9.8	4.9	2.0	12.1	6.0	2.0
S7	8.9	4.5	1.9	7.6	4.0	1.9	11.2	5.3	2.1
S8	9.3	4.9	1.9	11.2	6.2	1.8	11.0	6.1	1.7
S9	10.8	6.7	1.6	10.9	5.2	2.1	9.3	5.2	1.8
S10	9.7	4.8	2.0	10.2	7.8	1.3	12.5	6.5	1.9
S11	8.9	5.2	1.7	7.2	5.1	1.4	13.7	6.8	2.0
S12	9.3	6.6	1.4	11.3	6.6	1.7	11.7	7.3	1.6
S13	11.7	5.5	2.1	9.7	4.6	2.1	10.3	5.7	1.8
S14	12.9	6.4	2.0	12.6	6.6	1.9	9.7	5.1	1.9
S15	7.8	4.1	1.9	13.1	7.2	1.8	11.6	5.8	2.0
S16	9.4	6.2	1.5	8.9	5.9	1.5	12.6	7.4	1.7
S17	12.4	7.3	1.7	10.6	5.0	2.1	13.6	6.8	2.0
S18	11.8	5.9	2.0	11.3	5.9	1.9	10.9	6.8	1.6
S19	12.4	7.7	1.6	11.0	5.0	2.2	13.1	7.3	1.8
S20	13.4	7.0	1.9	12.2	6.4	1.9	11.2	5.1	2.2
S21	12.9	5.8	2.2	9.9	7.6	1.3	9.9	6.6	1.5
S22	11.6	6.4	1.8	8.9	4.9	1.8	11.7	5.8	2.0
S23	8.9	4.2	2.1	11.9	5.9	2.0	11.9	5.9	2.0
S24	10.9	7.3	1.5	9.7	6.0	1.6	9.9	5.8	1.7
S25	10.7	6.6	1.6	10.3	7.9	1.3	13.1	6.2	2.1
S26	11.7	5.8	2.0	12.5	5.6	2.2	12.1	6.0	2.0

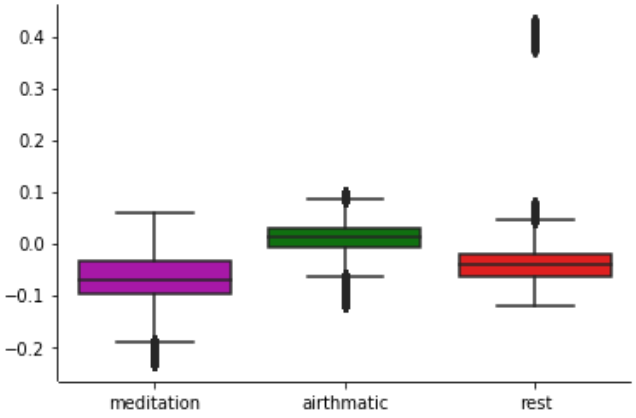

Figure 4 Box Plot of the data when the electrodes at Fp1 and Fp2 positions.

Similarly, Table 4 summarizes the peak frequencies in alpha and theta bands and their ratios when the positions of electrodes were at Af3 and Af4. From the below findings, it is evident that the cross-frequency corrilations (alpha: theta: 2.1) were maximum in the arithmetic state i.e. 11 times (for subjects S0, S3, S7, S8, S9, S13, S15, S18, S19, S23 and S25) and minimum in the case of meditation i.e. 2 times (for subjects S5 and S12) whereas, in the rest state, it has been found 7 times (for subjects S3, S6, S10, S13, S19, S20 and S24).
From these findings, it is clear that:

% of alpha-theta cross-frequency occurrences during arithmetic state= 11*100/27=40.74
% of alpha-theta cross-frequency occurrences during meditation state= 2*100/27=7.40
% of alpha-theta cross-frequency occurrences during rest state= 7*100/27=25.92

From the above calculations, it was observed that the occurrence of the cross-frequency is maximum in the arithmetic state, i.e., 40.74, and minimum in the case of the meditation state, i.e.7.40.

In contrast, the rest state is found in between these two states, i.e., 25.92. Thus the cross-frequency occurrence pattern hass been found as *Arithmetic> Rest>meditation*. The box plot of the dataset is shown in Figure 5. It can be observed that the mean values of the meditation and rest state data were found less than the arithmetic state data. Whereas the width of the meditation box and arithmetic box appear larger than the rest, suggesting that the data range of meditation and arithmetic was found more than the rest. The outlier values were also found in some states of the experiment. The source of these outliers has already been explained.

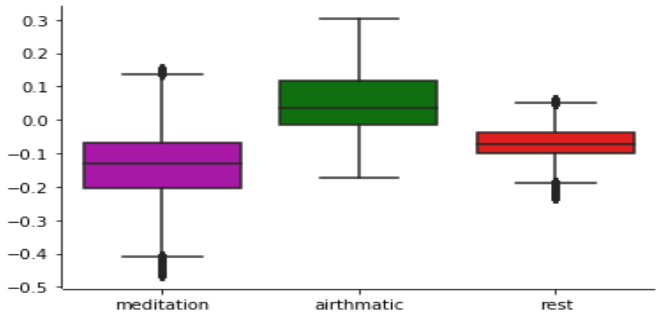

Figure 5 Box Plot of the data when the electrodes were at Af3 and Af4 positions.

Similarly, Table 5 illustrares the alpha and theta band frequencies' peak values and their ratios at the electrodes positions Af7 and Af8. The maximum occurrence of alpha-theta cross frequencies was found in the arithmetic state (nine times), while the resting and meditation states have seen the same number of cross-frequency occurances (five times) .

% of alpha-theta cross-frequency occurrences during arithmetic state= 9*100/27=33.33

% of alpha-theta cross-frequency occurrences during meditation state= 5*100/27=18.51

% of alpha-theta cross-frequency occurrences during rest state= 5*100/27=18.51

Table 4 Peak frequencies (in Hz) values (approx.) of alpha, theta bands, and their ratios in three different task conditions, the electrodes were placed at Af3, Af4 position.

Sub	Rest			Meditation			Arithmetic		
	α(M)	θ(M)	α(M)/θ(M)	α(M)	θ(M)	α(M)/θ(M)	α(M)	θ(M)	α(M)/θ(M)
S0	8.9	5.5	1.6	7.9	4.9	1.6	13.2	6.6	2.0
S1	11.2	5.8	1.9	9.2	4.8	1.9	12.3	6.8	1.8
S2	11.7	6.8	1.7	7.6	5.0	1.5	12.9	8.0	1.6
S3	9.3	4.6	2.0	8.9	5.5	1.6	11.9	5.9	2.0
S4	8.9	5.6	1.6	9.8	5.1	1.9	10.2	5.3	1.9
S5	11.2	6.5	1.7	10.1	5.0	2.0	10.6	6.6	1.6
S6	9.6	6.4	2.0	9.7	5.7	1.7	12.9	8.6	1.5
S7	10.3	5.7	1.8	10.9	7.2	1.5	11.8	5.9	2.0
S8	10.9	5.7	1.9	11.3	6.2	1.8	11.9	5.9	2.0
S9	11.3	6.6	1.7	12.1	7.5	1.6	12.3	6.1	2.0
S10	9.4	4.7	2.0	9.5	5.9	1.6	9.2	5.1	1.8
S11	10.7	5.6	1.9	7.2	4.0	1.8	8.1	4.2	1.9
S12	10.4	7.4	1.4	11.7	5.8	2.0	12.2	7.1	1.7
S13	11.1	5.5	2.0	12.2	6.4	1.9	11.5	5.7	2.0
S14	13.4	7.4	1.8	9.9	5.5	1.8	13.7	7.6	1.8
S15	7.9	5.6	1.4	10.5	5.0	2.1	11.2	5.6	2.0
S16	8.5	4.4	1.9	13.1	6.8	1.9	9.6	6.0	1.6
S17	9.7	6.9	1.4	8.9	6.8	1.3	8.7	6.0	1.4
S18	10.6	6.2	1.7	10.3	5.4	1.9	11.5	5.7	2.0
S19	12.5	6.2	2.0	7.6	4.7	1.6	11.8	5.9	2.0
S20	11.3	5.6	2.0	9.4	6.7	1.4	13.6	7.1	1.9
S21	9.0	5.6	1.6	10.9	6.4	1.7	9.8	5.7	1.7
S22	8.6	4.5	1.9	8.2	4.5	1.8	10.5	7.5	1.4
S23	7.6	5.8	1.3	11.9	7.0	1.7	11.6	5.8	2.0
S24	11.9	5.9	2.0	12.0	6.3	1.9	9.5	5.5	1.7
S25	12.3	6.8	1.8	9.5	5.5	1.7	10.8	5.5	2.0
S26	9.2	6.1	1.6	11.6	7.7	1.5	13.2	7.3	1.8

In this case, it was found that the maximum percentage of the cross-frequency is during the arithmetic condition (i.e. 33.33). At the same time, the meditation and resting states both have the same percentage of occurrence of cross-frequency, i.e., 18.51. Thus the cross-frequency occurrence pattern was found *Arithmetic>rest=meditation*. The box plot of the dataset is also shown in Figure 6. It can be observed that the mean values of the meditation and resting state data were found less than the arithmetic state data. While the width of the rest box seems more than the remaining two boxes, which indicates the data range of the rest state is more than the other two.

The findings revels that at all the three positions (i.e. Fp1, Fp2, Af3, Af4, Af7 and Af8) the maximum number of cross-frequency occurrences has been found in the case of arithmetic state The theta values are constantly lower in all three positions in the meditation state while the alpha values are constantly high in the arithmetic state.

Secondary analysis: In the secondary approach**,** the authors simultaneously compared the ERPs and SPDs under different task conditions for all 27 test subjects.

ERP-based comparisons: After a comparative study of peak alpha, theta, and cross frequency corrilations of the individual test subject, the study of all 27 subjects was created in EEGLAB. The comparisons were carried out about the ERPs and PSDs for all 27 subjects, and the comparison results are shown in the figures. The study creation option in EEGLAB provides us to analyze the group dataset simultaneously. An EEGLAB study contains a description and links to data contained in many epoched or continuous data sets, such as A set of the dataset from a group of subjects in one or more conditions of the same task or performing different tasks in the same or different sessions. A study may be created to manage and process the data recorded from multiple subjects, sessions, and conditions of an experimental study.

Table 5 Peak frequencies (approx.) of alpha-theta and their ratios in three different states (rest, meditation, and arithmetic), the electrodes were placed at Af7, Af8 positions.

Sub:	Rest			Meditation			Arithmetic		
	α(M)	θ(M)	α(M)/θ(M)	α(M)	θ(M)	α(M)/θ(M)	α(M)	θ(M)	α(M)/θ(M)
S0	10.1	5.9	1.7	7.5	4.1	1.8	12.3	6.1	2.0
S1	11.0	6.8	1.6	8.3	4.1	2.0	13.2	6.2	2.1
S2	8.9	4.6	1.9	7.9	4.1	1.9	13.7	7.2	1.9
S3	9.2	4.6	2.0	9.1	5.6	1.6	11.8	7.3	1.6
S4	7.8	4.3	1.8	10.4	6.9	1.5	10.2	6.8	1.5
S5	7.4	4.1	1.8	9.9	5.5	1.8	9.9	5.5	1.8
S6	8.4	4.2	2.0	10.2	5.6	1.8	10.0	5.0	2.0
S7	8.2	5.4	1.5	10.3	6.4	1.6	11.7	6.1	1.9
S8	11.2	6.5	1.7	11.2	7.0	1.6	12.8	6.4	2.0
S9	12.0	6.3	1.9	7.5	4.6	1.6	11.7	7.3	1.6
S10	11.1	6.1	1.8	9.6	4.8	2.0	9.8	6.5	1.5
S11	8.8	5.5	1.6	11.2	6.5	1.7	10.5	6.1	1.7
S12	13.0	6.5	2.1	13.4	7.4	1.8	8.9	4.6	1.9
S13	11.8	6.2	1.9	9.2	5.7	1.6	11.2	5.6	2.0
S14	11.2	7.2	1.5	8.7	4.1	2.1	11.7	5.8	2.0
S15	10.4	5.5	1.8	12.4	6.2	2.0	13.6	6.4	2.1
S16	11.6	5.8	2.0	11.9	7.4	1.6	8.3	5.5	1.5
S17	9.1	4.8	1.8	13.2	6.6	2.0	12.6	7.0	1.8
S18	8.9	4.6	1.9	9.0	4.7	1.9	11.9	5.9	2.0
S19	13.5	7.9	1.7	9.7	5.7	1.7	8.9	4.6	1.9
S20	8.4	4	2.1	10.8	7.2	1.5	7.6	4.7	1.6
S21	7.3	4.8	1.5	10.1	5.0	2.0	11.1	5.5	2.0
S22	9.0	6.9	1.3	8.3	4.6	1.8	13.7	7.2	1.9
S23	10.7	6.2	1.7	13.4	7.0	1.9	9.0	6.4	1.4
S24	11.4	5.7	2.0	7.8	6.0	1.3	12.3	6.1	2.0
S25	10.6	5.3	2.0	8.6	5.0	1.7	7.9	4.6	1.7
S26	9.5	6.7	1.4	10.8	7.2	1.5	12.6	6.3	2.0

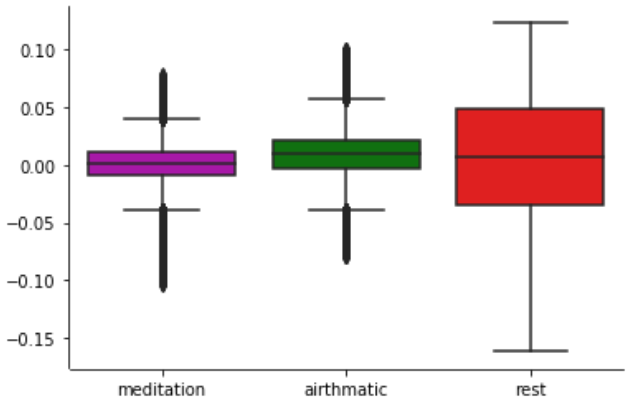

Figure 6 Box Plot of the dataset when the electrodes at Af7 and Af8 positions.

The present study provided the toolbox of 27 test persons with three states (arithmetic, meditation, and rest).

After uploading all the data in a SET file format, the options for comparing Power Spectral Density (PSD) and event-related potentials (ERP) concerning frequency and time are available. The analysis shows the differences among the three conditions, i.e., rest, arithmetic, and meditation.

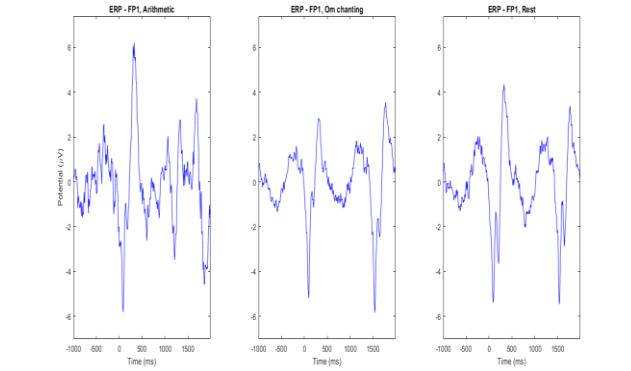

(a)

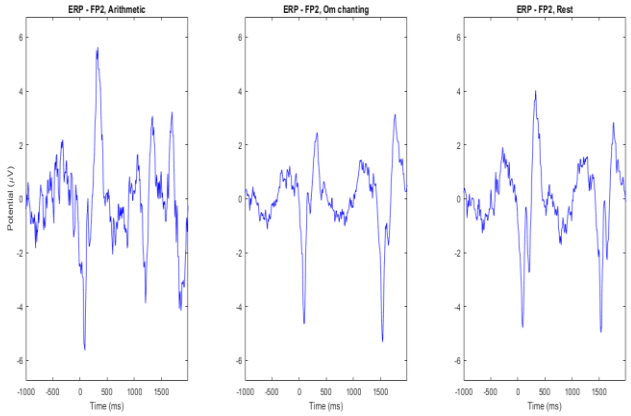

(b)

Figure 7 illustrates the ERP vs time variations in three different states (rest, meditation, arithmetic) (a) at Fp1 (b) at Fp2

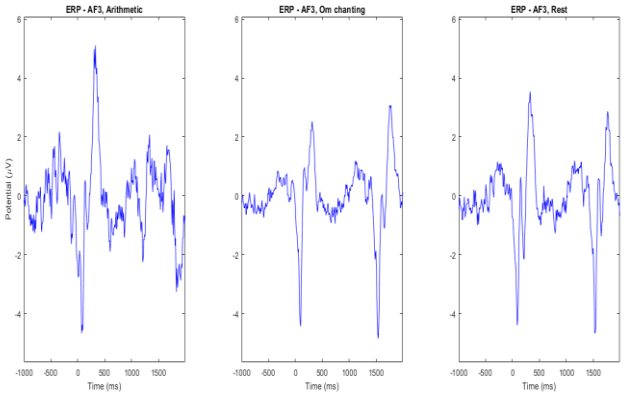

(a)

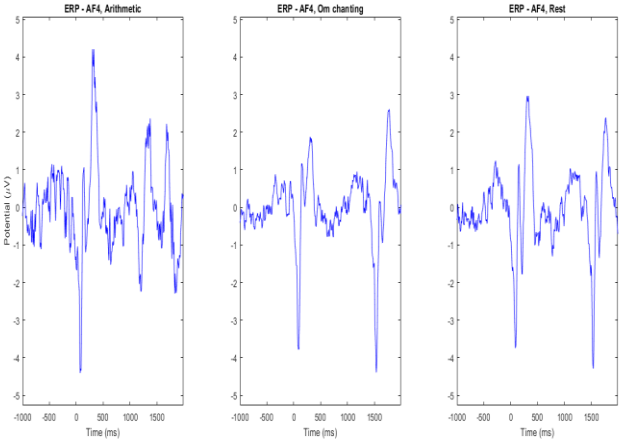

(b)

Figure 8 illustrates the ERP vs time variations in three different states (rest, meditation, arithmetic) (a) at Af3 (b) at Af4

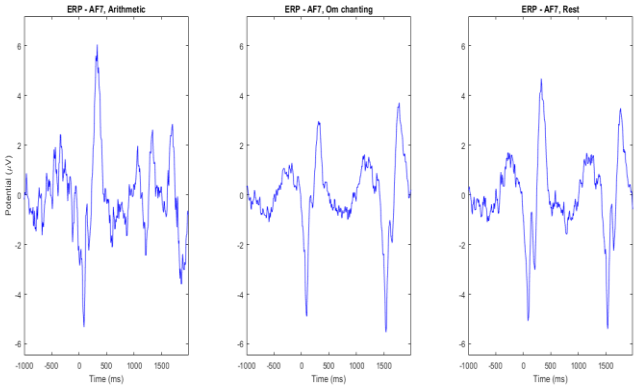

(a)

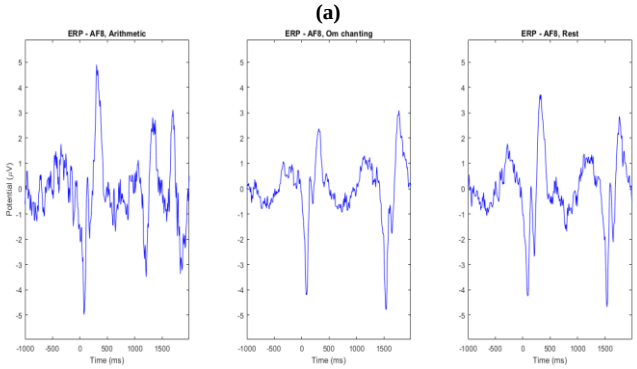

(b)

Figure 9 illustrates the ERP vs time variations in the three different states (rest, meditation, arithmetic) (a) at Af7 (b) at Af8

The ERP-based study analysis shows that the maximum values of ERPs were reported during an arithmetic operations. The ERP values are higher than the rest and meditation (at all the electrode positions). A comparison between the meditation state and rest has shown that the meditation state is more sluggish than the rest state. The Table 6 illusttes the maximum variations in ERPs in different electrode postions. The maximum variations have been seen in the arithmetic positions irrespective to all electrode positions. The ERPs in rest positions were found in between the arithmetic and meditation states. In the meditation state the ERPs were found low in all the electrode positions. It clearly indicates that the meditation state is sluggish than the rest and arithmetic states.

Table 6 Peak ERPs during different task conditions

Electrode posiions	Task state	Peak (approx.) ERP values
Fp1, Fp2	Arithmetic	6.1, 5.9
	Rest	4.2, 4.0
	Meditation	3.7, 3.2
Af3,Af4	Arithmetic	4.9, 4.2
	Rest	3.4, 3
	Meditation	2.8, 2.7
Af7,Af8	Arithmetic	6.0, 5.0
	Rest	3.9, 4.9
	Meditation	3.9, 2.9

PSD-based comparisons: When analyzing the power spectral densities (PSDs) of the three different states, it has been found that the peak PSD values occurred during the arithmetic state. The arithmetic state PSD values were slightly higher in comparison to the other two states, i.e., rest and meditation, whereas in rest and meditation states the results were approximately similar. In comparing PSD between meditation and rest state, it has been found that human brain was more relaxed in the state of meditation and this state was more sluggish than the other two.

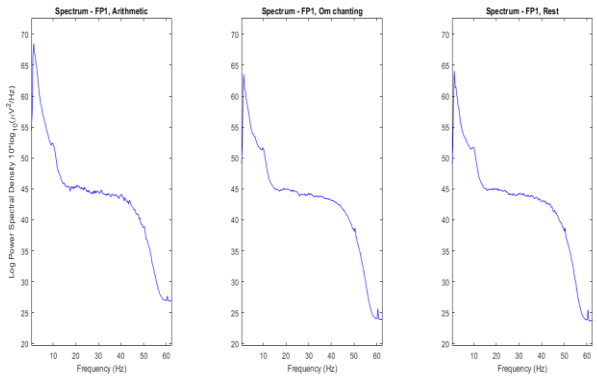

(a)

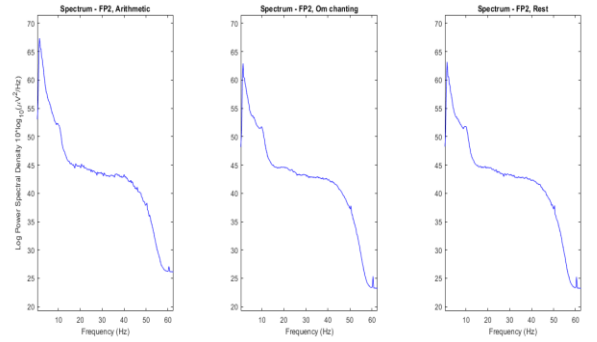

(b)

Figure 10 PSD vs frequency variations in the three different states (rest, meditation, arithmetic) (a) Fp1 (b) Fp2

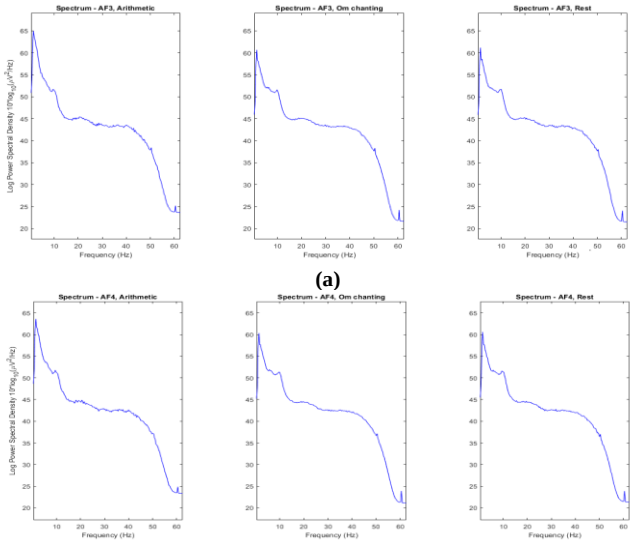

(a)

(b)

Figure 11 PSD vs frequency variations in the three different states (rest, meditaion, arithmetic) (a) Af3 (b) Af4

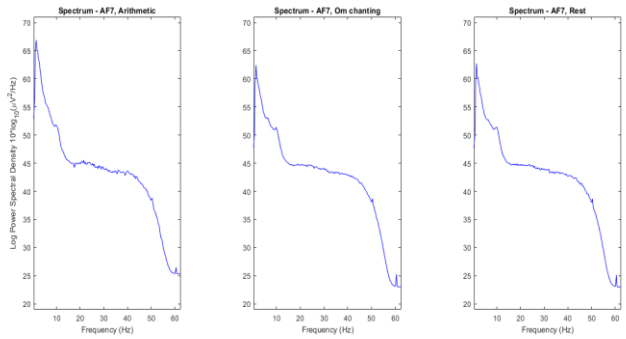

(a)

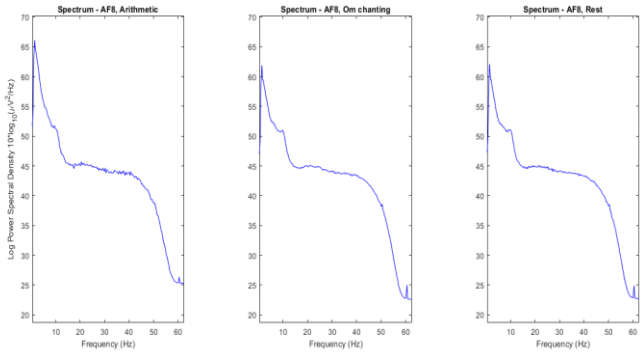

(b)

Figure 12 PSD vs frequency variations in the three different states (rest, meditation, arithmetic) (a) Af7 (b) Af8

In Figure 10, at positions Fp1, Fp2 the PSD (peak values) of 68 and 67 were found in the arithmetic state, while these values lie between 60 and 65 in the resting and meditation states. Similarly in Figure 11 PSD peaks were 65 and 64 at positions Af3, Af4 during the arithmetic task, while the rest and meditation-related PSD were slightly lower, i.e., close to 60. In Figure 12, similar patterns were found when the electrodes were placed at Af7 and Af8, , i.e., the maximum value of the PSD in the case of the arithmetic state and the resting and meditation states showing fewer PSD values. In most of these cases, a steep drop is seen after the frequency of 40 Hz.

DISCUSSION

This study examined the transient relationship (alpha: theta: 2:1) during different states of the brain (i.e., rest, arithmetic, meditation) for a designed cognitive task. The analysis results suggested that during arithmetic conditions, transient alpha-theta (2:1) were found more frequently than the other two states (i.e., rest and meditation). Also, the peak values of alpha and theta appeared high during the arithmetic state. The experiment focused mainly on the frontal lobe. The entire-brain region has been considered in previous studies and types of literature [28, 40]. Brain oscillations are non-stationary, so the condition of this transient relationship between alpha and theta peak values was instantaneous [41, 42]. The study suggested that the increase in cognitive demand (i.e., arithmetic) significantly increases the occurrences of alpha-theta transient relationship for their peak frequencies. Previous studies illustrated that the transient alpha-theta corrilation-based comparison for arithmetic and rest conditions increased the frontal region's activity. In contrast, the central and left temporoparietal region was found more activated for rest and meditation conditions. The transient arithmetic relationship was found in the frontal area [28]. Working memory and execution control has been related to the cognitive demand of the experiment [43-45], It can be correlated that the maximum manipulation and execution in mind were during arithmetic operation [46-49] and during meditation state, the same manipulation and execution has been found less because the brain was trying to be calm or mental emptiness [50-52]. The overall conclusion was that alpha-theta cross-frequency appearance for the three different conditions in a manner viz: arithmetic>aest>meditation [28]. In our experiment, Om chanting sound (963Hz) has been used to achieve mental emptiness instead of meditation practice. Here, manipulation and execution happened in the rest condition but less than the arithmetic state.

Previous studies suggest that the maximum occurrences of the alpha-theta cross-frequency relationship happen when the alpha

range is 11-12 Hz, and the theta range is 4-6 Hz [28, 53]. The authors claim comparable results with the six electrodes on the frontal lobe. Findings also indicated maximum episodes where the cross-frequency relationship occurred (in arithmetic conditions) with alpha values between 9-12 Hz. A previous work illustrated that effortful cognition increased the alpha peaks frequency [54], decreases theta peak frequency [28], and an increase in alpha-theta cross-frequency relationship [55]. The author presents maximum numbers of cross-frequency alpha-theta corrilations in arithmetic conditions (at all electrode positions). Another insight reflected that maximum alpha-theta cross-frequency episodes were found when the electrodes were placed at Af3, and Af4 positions, indicating that Af3 and Af4 positions are maximally involved in the task process than the other two electrodes positions. In the ERP and PSD comparisons, the maximum variations in arithmetic conditions and the maximum peak values of PSD in arithmetic state also supported the previous studies. The result suggests that neural oscillations related to the arithmetic condition are higher than the other two (i.e., rest and meditation).

CONCLUSION

The experiment outcomes demonstrate how the alpha-theta cross-frequency varies with the different mental states. The cross-frequency corrilations between alpha theta rhymes were enhanced during an effortful cognitive task, whereas it decreases at the state of meditation. This work analyzes and distinguishes the various states of mind during a designed cognitive task (rest, arithmetic, and induced meditation). The participants induced the meditation by listening to OM chanting of 963 Hz, i.e., the crown chakra frequency. The arithmetic operation was a simple mathematical problem. The study concluded that alpha theta cross-frequency occurrences were maximum during arithmetic operation, i.e., 33%, 40.74%, and 33.33%. The alpha theta cross-frequency in the rest state is lower than the arithmetic task, i.e., 22.22%, 25.92%, and 18.51%. Moreover, the Alpha theta cross-frequency in the meditation state is lower than the rest state, i.e., 7.40%, 7.40%, and 18.51%. The study concluded that cross-frequency corrilations were enhanced during effortful cognition, whereas it decreases at the state of mental emptiness. It was found that alpha-theta cross-frequency occurrences are 40.74% (maximum) when electrodes are placed at Af3 and Af4. The comparisons based on ERPs and PSDs have also been introduced for the subjects. The results showed that the meditation state is more sluggish than the arithmetic and rest one. In the future, upcoming researchers may be used this approach to classify the different states of brain and an EEG-based dual-channel device could also be framed in the form of hardware. The task may be redesigned with more different states of brain.

References

1. Shapiro Jr, Deane H. *Meditation: Self-regulation strategy and altered state of consciousness*. Routledge, 2017.
2. Bryant, Fred B., and Joseph Veroff. *Savoring: A new model of positive experience*. Psychology Press, 2017.
3. Grossenbacher, Peter G., and Jordan T. Quaglia. "Contemplative cognition: A more integrative framework for advancing mindfulness and meditation research." *Mindfulness* 8.6 (2017): 1580-1593.
4. Deolindo, Camila Sardeto, *et al*. "A critical analysis on characterizing the meditation experience through the electroencephalogram." *Frontiers in Systems Neuroscience* 14 (2020): 53.
5. Reinhart, Robert MG, and John A. Nguyen. "Working memory revived in older adults by synchronizing rhythmic brain circuits." *Nature neuroscience* 22.5 (2019): 820-827.
6. Spooner, Rachel K., *et al*. "Prefrontal theta modulates sensorimotor gamma networks during the reorienting of attention." *Human brain mapping* 41.2 (2020): 520-529.
7. Reteig, Leon C., *et al*. "Sustaining attention for a prolonged period of time increases temporal variability in cortical responses." *Cortex* 117 (2019): 16-32.
8. Siegel, Daniel. *Aware: The science and practice of presence--the groundbreaking meditation practice*. TarcherPerigee, 2020.
9. Rogers, Holly, and Margaret Maytan. *Mindfulness for the next generation: Helping emerging adults manage stress and lead healthier lives*. Oxford University Press, 2019.
10. Cohen, Kenneth S. *The way of qigong: The art and science of Chinese energy healing*. Wellspring/Ballantine, 2018.
11. He, Bin, *et al*. "Electrophysiological source imaging: a noninvasive window to brain dynamics." *Annual review of biomedical engineering* 20 (2018): 171-196.
12. Davis, Jeffrey Jonathan Joshua, *et al*. "An integrative approach to analyze EEG signals and human brain dynamics in different cognitive states." *Journal of Artificial Intelligence and Soft Computing Research* 7.4 (2017): 287-299.
13. Seleznov, Ivan, *et al*. "Detrended fluctuation, coherence, and spectral power analysis of activation rearrangement in EEG dynamics during cognitive workload." *Frontiers in human neuroscience* 13 (2019): 270.
14. Rodriguez-Larios, Julio, and Kaat Alaerts. "EEG alpha–theta dynamics during mind wandering in the context of breath focus meditation: An experience sampling approach with novice meditation practitioners." *European Journal of Neuroscience* 53.6 (2021): 1855-1868.
15. Kam, Julia WY, *et al*. "Lateral prefrontal cortex lesion impairs regulation of internally and externally directed attention." *Neuroimage* 175 (2018): 91-99.
16. Song, Tengfei, *et al*. "MPED: A multi-modal physiological emotion database for discrete emotion recognition." *IEEE Access* 7 (2019): 12177-12191.
17. Popov, T. *et al*. Cross-frequency interactions between frontal theta and posterior alpha control mechanisms foster working memory. Neuroimage 181, 728–733 (2018).
18. Portoles, Oscar, Jelmer P. Borst, and Marieke K. van Vugt. "Characterizing synchrony patterns across cognitive task stages of associative recognition memory." *European Journal of Neuroscience* 48.8 (2018): 2759-2769.
19. Chung, Sung Wook, *et al*. "Impact of different intensities of intermittent theta burst stimulation on the cortical properties during TMS-EEG and working memory performance." *Human Brain Mapping* 39.2 (2018): 783-802.
20. Magosso, Elisa, *et al*. "EEG alpha power is modulated by attentional changes during cognitive tasks and virtual reality immersion." *Computational intelligence and neuroscience* 2019 (2019).

21. Rodriguez-Larios, Julio, and Kaat Alaerts. "Tracking transient changes in the neural frequency architecture: harmonic relationships between theta and alpha peaks facilitate cognitive performance." *Journal of Neuroscience* 39.32 (2019): 6291-6298.
22. Kakumanu, Ratna Jyothi, *et al*. "Dissociating meditation proficiency and experience dependent EEG changes during traditional Vipassana meditation practice." *Biological psychology* 135 (2018): 65-75.
23. Nair, Ajay Kumar, *et al*. "Just a minute meditation: Rapid voluntary conscious state shifts in long term meditators." *Consciousness and cognition* 53 (2017): 176-184.
24. Sharma, Kanishka, Sushil Chandra, and Ashok Kumar Dubey. "Exploration of lower frequency EEG dynamics and cortical alpha asymmetry in long-term rajyoga meditators." *International journal of yoga* 11.1 (2018): 30.
25. Harne, Bhavna P., and A. S. Hiwale. "EEG spectral analysis on OM mantra meditation: A pilot study." *Applied psychophysiology and biofeedback* 43.2 (2018): 123-129.
26. Kakumanu, Ratna Jyothi, *et al*. "Dissociating meditation proficiency and experience dependent EEG changes during traditional Vipassana meditation practice." *Biological psychology* 135 (2018): 65-75.
27. Irrmischer, Mona, *et al*. "Controlling the temporal structure of brain oscillations by focused attention meditation." *Human brain mapping* 39.4 (2018): 1825-1838.
28. Baranski, Michael FS, and Christopher A. Was. "A more rigorous examination of the effects of mindfulness meditation on working memory capacity." *Journal of Cognitive Enhancement* 2.3 (2018): 225-239.
29. Rodriguez-Larios, Julio, *et al*. "From thoughtless awareness to effortful cognition: alpha-theta cross-frequency dynamics in experienced meditators during meditation, rest and arithmetic." *Scientific reports* 10.1 (2020): 1-11.
30. Davies, Brenda. *The 7 Healing Chakras: Unlocking Your Body's Energy Centers*. Ulysses Press, 2021.
31. Myss, Caroline. *Anatomy of the spirit: The seven stages of power and healing*. Harmony, 2013.
32. Steinhorn, David M., Jana Din, and Angela Johnson. "Healing, spirituality and integrative medicine." *Ann Palliat Med* 6.3 (2017): 237-47.
33. Means, Barbara. "Cognitive task analysis as a basis for instructional design." *Cognitive science foundations of instruction*. Routledge, 2020. 97-118.
34. Greeno, James G. "Some examples of cognitive task analysis with instructional implications." *Aptitude, learning, and instruction*. Routledge, 2021. 1-22.
35. Means, Barbara. "Cognitive task analysis as a basis for instructional design." *Cognitive science foundations of instruction*. Routledge, 2020. 97-118.
36. Crandall, Beth, *et al*. *Working minds: A practitioner's guide to cognitive task analysis*. Mit Press, 2006.
37. Stanton, Neville Anthony, *et al*., eds. *Handbook of human factors and ergonomics methods*. CRC press, 2004.
38. Sazgar, Mona, and Michael G. Young. "Overview of EEG, electrode placement, and montages." *Absolute epilepsy and EEG rotation review*. Springer, Cham, 2019. 117-125.
39. Sazgar, Mona, and Michael G. Young. "EEG artifacts." *Absolute epilepsy and EEG rotation review*. Springer, Cham, 2019. 149-162.
40. Cohen, M. X. Fluctuations in Oscillation Frequency Control Spike Timing and Coordinate Neural Networks. J. Neurosci. 34, 8988–8998 (2014).
41. Rodriguez-Larios, Julio, and Kaat Alaerts. "Tracking transient changes in the neural frequency architecture: harmonic relationships between theta and alpha peaks facilitate cognitive performance." *Journal of Neuroscience* 39.32 (2019): 6291-6298.
42. Rodriguez-Larios, Julio, *et al*. "Mindfulness training is associated with changes in alpha-theta cross-frequency dynamics during meditation." *Mindfulness* 11.12 (2020): 2695-2704.
43. Mierau, Andreas, Wolfgang Klimesch, and Jérémie Lefebvre. "State-dependent alpha peak frequency shifts: Experimental evidence, potential mechanisms and functional implications." *Neuroscience* 360 (2017): 146-154.
44. Marvel, Cherie L., Owen P. Morgan, and Sharif I. Kronemer. "How the motor system integrates with working memory." *Neuroscience & Biobehavioral Reviews* 102 (2019): 184-194.
45. Matysiak, Olga, Aleksandra Kroemeke, and Aneta Brzezicka. "Working memory capacity as a predictor of cognitive training efficacy in the elderly population." *Frontiers in aging neuroscience* 11 (2019): 126.
46. Takeuchi, Hikaru, *et al*. "General intelligence is associated with working memory-related brain activity: new evidence from a large sample study." *Brain Structure and Function* 223.9 (2018): 4243-4258.
47. Cragg, Lucy, *et al*. "When is working memory important for arithmetic? The impact of strategy and age." *PLoS One* 12.12 (2017): e0188693.
48. Caviola, Sara, *et al*. "Stress, time pressure, strategy selection and math anxiety in mathematics: A review of the literature." *Frontiers in psychology* 8 (2017): 1488.
49. Hsieh, L.-T. & Ranganath, C. Frontal midline theta oscillations during working memory maintenance and episodic encoding and retrieval. 85 (2014).
50. Williams, C. C., Kappen, M., Hassall, C. D., Wright, B. & Krigolson, O. E. Thinking theta and alpha: Mechanisms of intuitive and analytical reasoning. Neuroimage 189, 574–580 (2019).
51. Garrison, K. A. *et al*. Effortless awareness: using real time neurofeedback to investigate correlates of posterior cingulate cortex activity in meditators' self-report. Front. Hum. Neurosci. 7, 440 (2013).
52. Brewer, J. A. & Garrison, K. A. The posterior cingulate cortex as a plausible mechanistic target of meditation: Findings from neuroimaging. Ann. N. Y. Acad. Sci. 1307, 19–27 (2014)
53. Wahbeh, H., Sagher, A., Back, W., Pundhir, P. & Travis, F. A systematic review of transcendent states across meditation and contemplative traditions. Explore 14 (2018).
54. Axmacher, N. *et al*. Cross-frequency coupling supports multi-item working memory in the human hippocampus. Proc. Natl. Acad. Sci. USA 107, 3228–33 (2010).
55. Haegens, S., Cousijn, H., Wallis, G., Harrison, P. J. & Nobre, A. C. Inter- and intra-individual variability in

alpha peak frequency, https://doi.org/10.1016/ j.neuroimage.2014.01.049 (2014).
56. Dimitriadis, S. I., Sun, Y., Thakor, N. V. & Bezerianos, A. Causal Interactions between Frontalθ – Parieto-Occipitalα2 Predict Performance on a Mental Arithmetic Task. Front. Hum. Neurosci. 10, 454 (2016).
57. Lai-Wo Stan Leung, F.H.Lopes Da Silva, W.J Wadman, Spectral characteristics of the hippocampal EEG in the freely moving rat, Electroencephalography and Clinical Neurophysiology, Volume 54, Issue 2,1982,Pages 203-219,ISSN 0013-4694,